P-04-77

Oskarshamn site investigation

Interpretation of geophysical borehole data and compilation of petrophysical data from KSH02 (80–1000 m) and KAV01

Håkan Mattsson, Hans Thunehed
GeoVista AB

April 2004

Svensk Kärnbränslehantering AB
Swedish Nuclear Fuel
and Waste Management Co
Box 5864
SE-102 40 Stockholm Sweden
Tel 08-459 84 00
+46 8 459 84 00
Fax 08-661 57 19
+46 8 661 57 19

ISSN 1651-4416
SKB P-04-77

Oskarshamn site investigation

Interpretation of geophysical borehole data and compilation of petrophysical data from KSH02 (80–1000 m) and KAV01

Håkan Mattsson, Hans Thunehed
GeoVista AB

April 2004

Keywords: Borehole, Logging, Geophysics, Geology, Bedrock, Fractures, Salinity, Porosity, Temperature gradient.

Abstract

This report presents the compilation and interpretations of geophysical logging data and petrophysical measurements on rock samples from the cored boreholes KSH02 (the Simpevarp peninsula) and KAV01 (the Ävrö Island).

The main objective of these investigations is to use the results as supportive information during the geological core mappings and as supportive information during the single-hole interpretation. The petrophysical data are used to perform quality controls of the logging data and constitute supportive information to the rock type classification. Special emphasis was put on evaluating how plastic deformation and alteration affects the physical properties of the fine-grained dioritoid rock that dominates the bedrock of the Simpevarp peninsula.

The rock in the vicinity of KSH02 seems to be dominated by a rock type with a mineral composition that corresponds to tonalite or diorite rocks. The geophysical logging data indicate frequent occurrence of fine-grained granite and partly increased fracturing along the section 500–720 m. A possible deformation zone is also indicated at ca 280–300 m depth of KSH02. A prominent anomaly in the vertical temperature gradient data at 855 m depth might indicate the occurrence of a water bearing fracture.

The geophysical logging data of KAV01 indicate increased fracturing along large parts of the section 400–565 m depth. The rock in the vicinity of KAV01 is dominated by silicate densities ranging from indicated granite to tonalite mineral composition. The natural gamma radiation intensity is higher along the uppermost ca 135 m and also along the section ca 500–600 m of the borehole, than for the other parts of KAV01. This might reflect lithological variations.

On basis of the results from the petrophysical measurements of KSH02 we conclude that strong alteration clearly affects the physical properties of the fine-grained dioritoid rock. The alteration gives rise to decreased density, magnetization and electric resistivity whereas the porosity increases. Thus, several different geophysical methods can be used to identify and locate zones of intense alteration of the bedrock at, and close to, the Simpevarp peninsula.

Sammanfattning

Föreliggande rapport presenterar en sammanställning och tolkning av geofysiska borrhålsdata och petrofysiska data från kärnborrhålen KSH02 på Simpevarpshalvön och KAV01 på Ävrö.

Syftet med denna undersökning är framförallt att ta fram ett material som på ett förenklat sätt åskådliggör resultaten av de geofysiska loggningarna, s.k. generaliserade geofysiska loggar. Materialet används dels som stödjande data vid borrkärnekarteringen samt som underlag vid enhålstolkningen för respektive borrhål. Petrofysikdata används dels för att kontrollera kvaliteten på vissa geofysiska loggar och dels som ett stöd vid bergartsklassificeringen. Ett mål med denna undersökning var också att undersöka hur kraftig omvandling och plastisk deformation påverkar de fysikaliska egenskaperna hos finkornig dioritoid, den bergart som tros dominera berggrunden på Simpevarpshalvön.

Geofysiska data indikerar att berggrunden i närheten av KSH02 domineras av bergarter med en mineralsammansättning motsvarande tonalit till diorit. Stora delar av berget längs sektionen 500–720 m verkar utgöras av finkornig granit. Längs denna sektion finns också indikationer på bitvis förhöjd sprickfrekvens. En möjlig deformationszon indikeras både i sonic- och resistivitetsdata mellan ca 280 m och 300 m djup. På ca 855 m djup finns en kraftig anomali i den vertikala temperaturgradienten, vilket kan indikera en vattenförande sprickzon.

Den uppskattade sprickfrekvensloggen för KAV01 indikerar förhöjd sprickighet längs stora delar av sektionen 400–565 m. Variationer i silikatdensiteten indikerar att berggrunden i närheten av hålet domineras av bergarter med en mineralsammansättning motsvarande granit, granodiorit eller tonalit. Gammastrålningsnivån är tydligt högre längs de översta 135 m och längs sektionen ca 500–600 m av KAV01. Detta kan möjligen kopplas till litologiska variationer längs borrhålet.

Den petrofysiska undersökningen av prover från KSH02 visar entydigt att kraftig omvandling påverkar de fysikaliska egenskaperna hos den finkorniga dioritoiden. Parametrarna densitet, inducerad och remanent magnetisering samt elektrisk resistivitet sjunker alla avsevärt, medan porositeten stiger. Således bör ett flertal olika geofysiska metoder kunna användas för att finna, och uppskatta utbredningen av, områden i berggrunden på och kring Simpevarpshalvön som påverkats av kraftig omvandling.

Contents

1 Introduction

SKB performs site investigations for localization of a deep repository for high level radioactive waste. The site investigations are performed at two sites, Forsmark and Simpevarp. This document reports the results gained from the interpretation of borehole geophysical logging data from the cored boreholes KSH02 at the Simpevarp peninsula and KAV01 located on the Ävrö Island. A compilation of petrophysical data from measurements on 21 core samples from KSH02 and 15 core samples from KAV01 is also presented.

Generalized geophysical loggings related to lithological variations are presented together with indicated fracture loggings (including estimated fracture frequency) and possible alteration. Apparent porosity, vertical temperature gradient and estimated salinity loggings are also calculated. The logging measurements of KSH02 were conducted in 2003 by Rambøll /1/. The data from KAV01 is a combination of three separate logging performances in 1978 and 1986 by Malå GeoScience, and in 2003 by Rambøll.

The petrophysical determinations include magnetic susceptibility, remanent magnetization, anisotropy of magnetic susceptibility (AMS), density, porosity, electric resistivity and induced polarization. The measurements were performed at the laboratory of the Division of Applied Geophysics, Luleå University of Technology.

The interpretation presented in this report is performed by GeoVista AB in accordance with the instructions and guidelines from SKB (activity plan AP PS 400-03-060 and method description MD 221.003, SKB internal controlling documents) and under supervision of Leif Stenberg, SKB.

2 Objective and scope

The purpose of geophysical measurements in boreholes is to gain knowledge of the physical properties of the bedrock in the vicinity of the borehole. A combined interpretation of the "lithological" logging data silicate density, magnetic susceptibility and natural gamma radiation, together with petrophysical data makes it possible to estimate the physical signature of different rock types. The three loggings are generalized and are then presented in a simplified way in the borehole software WellCad. The location of major fractures and an estimation of the fracture frequency along the borehole are calculated by interpreting data from the resistivity loggings, the single point resistance (SPR), caliper-mean and sonic loggings.

The main objective of these investigations is to use the results as supportive information during the geological core mappings and as supportive information during the so called "single-hole interpretation", which is a combined borehole interpretation of core logging (Boremap) data, geophysical data and radar data.

The petrophysical data are used to perform quality controls of the logging data and constitute supportive information to the rock type classification. Rock fabric information and parameters related to grain size are also achieved from the petrophysical measurements. For KSH02 special emphasis was put on evaluating how plastic deformation and alteration affects the physical properties of the fine-grained dioritoid rock that dominates the bedrock of the Simpevarp peninsula. The samples were therefore collected from primary, deformed and altered sections of the core.

3 Equipment

3.1 Description of equipment for petrophysical measurements

The measurements of magnetic remanence were performed with a cryogenic DC-SQUID magnetometer from 2G Enterprises and the anisotropy of magnetic susceptibility (AMS), including the magnetic volume susceptibility, was measured with a KLY-3 Kappabridge from Geofyzika Brno. Masses for the density and porosity determinations were measured with a digital Mettler Toledo PG 5002. The electric resistivity and induced polarization measurements were performed by use of a two-electrode in-house equipment (Luleå University of Technology) /2/.

3.2 Description of equipment for analyses of logging data

The software used for the interpretation are WellCad v3.2 (ALT), which is mainly used for plotting, Grapher v4 (Golden Software), mainly used for plotting and some statistical analyses, and a number of in-house software developed by GeoVista AB on behalf of SKB.

4 Execution

4.1 Laboratory measurements

Preparations of the drill cores were performed by a technician at the laboratory of the Division of Applied Geophysics, Luleå University of Technology, according to the standard techniques used for example, in the preparation of samples for paleomagnetic analyses. The core samples are not oriented with reference to any co-ordinate system, there is only a mark indicating section up and section low. The remanence vectors and anisotropy orientations were therefore performed only with reference to the core. Declination data of these parameters are consequently meaningless but inclination variations may be possible to interpret if the borehole is sub-vertical. The dip of KSH02 is c. 85° and the dip of KAV01 is c. 88°, which probably is steep enough to allow a meaningful interpretation of inclination variations in both boreholes, with an accuracy of c. ±5°.

The general measuring technique of the borehole samples was as follows. Electric and induced polarization measurements were firstly performed. The sample was soaked in tap water according to MD 230.001 (SKB internal controlling document). The surface of the sample was gently dried with a piece of paper before the sample was mounted in the two-electrode sample holder. Measurements were performed with a saw-tooth current wave-form with the frequencies 0.1, 0.6 and 4 Hz. All measurements were done in direct sequence to avoid drying of the sample. Harmonics of the lower frequencies were used to correct for possible drift due to drying. The electric resistivity of the soaking water was measured at regular intervals and recorded. The procedure was repeated after soaking the samples in water where 125 g of NaCl had been dissolved in 5 kg of water.

Four 22 mm long specimens were then drilled of each core sample (perpendicularly to the core of KSH02 and parallel to the core of KAV01). AMS measurements were performed on all four specimens and a measurement of the remanent magnetization was performed on one specimen. All specimens plus, if possible, the remains of the core sample, were then assembled and the density (wet and dry) and porosity measurements were performed. The samples were soaked in water for 48 hours (or more) and the mass was measured in air and in water, which allows a calculation of the wet density. The samples were dried in an oven at 107°C for 48 hours and the mass was measured in air. The three mass measurements allow a calculation of the porosity. The sample volume was then calculated by the use of Archimedes principle, and the dry density was calculated by dividing the dry mass with the volume. The average sample volume for the density and porosity measurements is c. 100 cm^3.

Measurements of density and porosity were performed according to MD 160.002 (SKB internal controlling document). The instruction is written to conform to rock mechanical measurements on drill cores from deep drillings, where the density and porosity determinations are parts of other types of measurements, not directly relevant for the geological core logging. The time to dry and soak the samples (48 hours in this investigation) is e.g. shorter than what is recommended in MD 160.002.

Calibration of instruments for measurements of petrophysical parameters were performed in accordance to the manual for each instrument respectively.

4.2 Preparations of the data

4.2.1 Petrophysical data

The laboratory measurements of petrophysical parameters produce raw-data files in ascii, binary or Microsoft Excel formats. All data files were delivered via email from the laboratory at the Luleå University of Technology to GeoVista AB. The data were then rearranged and placed in Microsoft Excel files. Back-up files of all raw-data are stored both at GeoVista AB and at the laboratory.

Sample information for KSH02 is given in Table 4-1 and for KAV01 in Table 4-2.

Table 4-1. Sample information for KSH02.

depth co-ordinate (m)	rock type	comment
20.44	fine-grained dioritoid	primary
148.68	fine-grained dioritoid	primary (weak alteration)
204.81	fine-grained dioritoid	primary
290.01	fine-grained dioritoid	strong alteration
290.94	fine-grained dioritoid	strong alteration
299.16	fine-grained dioritoid	strong alteration
358.08	fine-grained dioritoid	primary
385.66	fine-grained dioritoid	foliated
386.43	fine-grained dioritoid	foliated
402.32	fine-grained dioritoid	strong alteration
426.93	fine-grained dioritoid	primary
476.15	fine-grained dioritoid	primary
519.00	fine-grained dioritoid	strong alteration
522.81	fine-grained dioritoid	strong alteration
585.71	fine-grained dioritoid	primary (weak alteration)
681.01	fine-grained dioritoid	primary
753.28	fine-grained dioritoid	lineation
821.96	fine-grained dioritoid	primary
975.20	mafic volcanite	
976.30	mafic volcanite	
977.23	mafic volcanite	

Table 4-2. Sample information for KAV01.

depth co-ordinate (m)	rock type	comment
16.58	Fine-grained dioritoid	basic volcanite?
26.55	Ävrö granite	
70.23	Ävrö granite	
78.08	Fine-grained dioritoid	basic volcanite?
106.08	Ävrö granite	
170.13	Fine-grained dioritoid	granitic
200.23	Ävrö granite	
364.08	Fine-grained dioritoid	
415.38	Ävrö granite	
520.68	Ävrö granite	
610.08	Fine-grained dioritoid	
650.88	Fine-grained dioritoid	basic volcanite?
716.05	Ävrö granite	

4.2.2 Logging data of KSH02

The logging data were delivered as a Microsoft Excel file via email from Leif Stenberg, SKB. The data used for interpretation are:

- Density (gamma-gamma).
- Magnetic susceptibility.
- Natural gamma radiation.
- Focused resistivity (300 cm).
- Sonic.
- Caliper mean.
- Fluid resistivity.
- Fluid temperature.

The levels of the gamma-gamma and magnetic susceptibility loggings were adjusted by use of petrophysical data (see chapter 5.2.2). No normal, lateral resistivity or SPR measurements were performed in the borehole.

4.2.3 Logging data of KAV01

Data from three different logging performances were used in the analyses of KAV01. Some of the loggings only cover parts of the borehole. The logging data used for interpretation of KAV01 are:

- Lateral resistivity (Malå GeoScience, 1978), section: 22–492 m.
- Long normal resistivity, (Malå GeoScience, 1986), section: 3–741 m.
- SPR (Malå GeoScience, 1986), section: 10–743 m.
- Magnetic susceptibility (Malå GeoScience, 1986), section: 13–744 m.

- Natural gamma radiation (Malå GeoScience, 1986), section 2–743 m (used only for length adjustment).
- Fluid resistivity (Malå GeoScience, 1986), section 28–725 m (used for salinity calculation and correction of the long normal resistivity).
- Fluid temperature (Malå GeoScience, 1986), section 14–725 m (used as reference to the 2003 data).
- Fluid resistivity (Rambøll, 2003), section: 2–745 m (used as reference and control of older data).
- Fluid temperature (Rambøll, 2003), section: 2–745 m.
- Gamma-gamma (density) (Rambøll, 2003), section: 3–743 m.
- Natural gamma radiation (Rambøll, 2003), section: 1–745 m.
- Caliper mean (Rambøll, 2003), section: 2–743 m.

The older loggings (from 1978 and 1986) were extracted from the SKB database SICADA. Old logging data in SICADA are not length adjusted so these data were length adjusted in the following steps: first the 1978 lateral resistivity was adjusted with respect to the normal resistivity from 1986. Then, all old logging data were adjusted with the old geological core logging (petrocore) as reference. This step was followed by a cross matching between the old and the 2003 natural gamma radiation loggings, which leveled the old and the 2003 data with each other. As a final step, the gamma-gamma logging was length adjusted 0.3 m upwards with reference to the natural gamma radiation logging from 2003.

At 67.6 m depth the borehole diameter rapidly decreases (downward direction) from c. 170 mm to 58 mm. The caliper mean data are very noisy along the upper 67.6 m and were therefore disregarded in the fracture analysis. The signal level of the gamma-gamma, natural gamma and magnetic susceptibility loggings are clearly affected by this change in diameter, for which no compensation has been made for by the logging contractor. The levels of the gamma-gamma and magnetic susceptibility loggings were adjusted by use of petrophysical data (see chapter 5.2.3). The lack of radiation data in the petrophysical database calls for another way to “adjust” the level of the radiation logging. With reference to the old geological core logging (petrocore) the median natural gamma radiation values of two 5 m long sections, above and below the break at 67.6 m were calculated. The data from above 67.6 m were then adjusted for the quotient between the median values.

4.3 Interpretation of the logging data

The execution of the interpretation can be summarized in the following four steps:

1. Preparations of the logging data (calculations of noise levels, median filtering, error estimations, re-sampling, drift correction, length adjustment, correction of resistivity loggings for fluid resistivity and borehole diameter, calculation of apparent porosity, calculation of salinity, calculation of vertical temperature gradient).

The loggings are median filtered (generally 5 point filters for the resistivity loggings and 3 point filters for other loggings) and re-sampled to common depth co-ordinates (0.1 m point distance). The data of the resistivity loggings are corrected for the influence of the borehole diameter and the borehole fluid resistivity. The apparent porosity is calculated during the

correction of the resistivity loggings. The calculation is based on Archie's law; $\sigma = a\ \sigma_w\ \varphi^m + \sigma_s$ where σ = bulk conductivity (S/m), σ_w = pore water conductivity (S/m), φ = volume fraction of pore space, σ_s = surface conductivity (S/m) and "a" and "m" are constants. A least squares curve fit on resistivity and porosity data measured on rock samples is required to determine the three unknown constants "a", "m" and "σ_s". Curve fits were performed on the petrophysical resistivity and porosity data presented in this report. Since "a" and "m" vary significantly with variations in the borehole fluid resistivity, different estimations of the constants had to be performed with reference to the actual fluid resistivity in each borehole respectively. Only the long normal resistivity of KAV01 was corrected. The estimated constants are presented in Table 5-1, section 5.1.2.

The vertical temperature gradient (in degrees/km) is calculated from the fluid temperature logging for 9 meter sections according to the following equation /3/:

$$TempGrad = \frac{1000\left[9\sum zt - \sum z \sum t\right]\sin\varphi}{9\sum z^2 - \left(\sum z\right)^2}$$

where z = depth co-ordinate (m), t = fluid temperature (°C) and φ = borehole inclination (°).

The estimated water salinity is calculated as ppm NaCl in water following the simple relation from Crain's Petrophysical Handbook where:

$$WS = \frac{400000}{\left(1.8t + 32\right)^{0.88}\sqrt{\rho}}$$

WS = Water salinity (ppm NaCl), t = temperature (°C) and ρ = resistivity (Ωm).

2. Interpretation rock types (generalization of the silicate density, magnetic susceptibility and natural gamma radiation loggings)

The silicate density is calculated with reference to /4/ and the data are then divided into 5 sections indicating a mineral composition corresponding to granite, granodiorite, tonalite, diorite and gabbro rocks, according to /5/. The sections are bounded by the threshold values

granite < 2680 kg/m^3
2680 kg/m^3 < granodiorite < 2730 kg/m^3
2730 kg/m^3 < tonalite < 2800 kg/m^3
2800 kg/m^3 < diorite < 2890 kg/m^3
2890 kg/m^3 < gabbro

The magnetic susceptibility logging is subdivided into steps of decades and the natural gamma radiation is divided into "low", "medium" or "high" radiation, where the threshold values for each level are adjusted with respect to the geological environment at the measurement site.

A "possible alteration logging" is estimated by identifying sections along the boreholes where the silicate density, natural gamma radiation and magnetic susceptibility simultaneously lay below certain threshold values. The threshold values were determined by analyzing logging data from KSH01A from sections where the geological core mapping indicates various degrees of alteration /6/. The applied threshold values are:

silicate density ≤ 2800 kg/m^3
natural gamma radiation ≤ 20 μR/h
magnetic susceptibility ≤ 0.003 SI

3. Interpretation of the position of large fractures and estimated fracture frequency (classification to fracture logging and calculation of the estimated fracture frequency logging are based on analyses of the long normal resistivity, caliper mean, single point resistance and lateral resistivity for KAV01 and on sonic, caliper mean and focused resistivity (300 cm) for KSH02.

The position of large fractures is estimated by applying a second derivative filter to the logging data and then locating maxima (or minima depending on the logging method) in the filtered logging. Maxima (or minima) above (below) a certain threshold value (Table 4-3) are selected as probable fractures. The result is presented as a column diagram where column height 0 = no fracture, column height 1 = fracture indicated by one logging method, column height 2 = fracture indicated by two logging methods and so on. The estimated fracture frequency is calculated by applying a power function to the weighted sum (Table 4-3) of the maxima (minima) derivative loggings. Power functions have previously been estimated by correlating the weighted sum to the mapped fracture frequency in the cored borehole KSH01A and in the percussion drilled borehole HSH02 /6/. Since no resistivity methods were used in KSH02 the power function used for estimating the fracture frequency had to be adjusted. This was done by calculating a new power function based on the data from KSH01A using only the three methods that were measured in KSH02. The power function used in this study for KSH02 is:

Estimated fracture frequency = 2.37 (weighted sum)$^{0.66}$.

The complicated situation for KAV01, with different logging methods along the three sections 0–70 m (methods: lateral resistivity, long normal resistivity and SPR), 70–490 m (methods: lateral resistivity, long normal resistivity, SPR and caliper mean) and 490–750 m (methods: long normal resistivity, SPR and caliper mean), makes it fairly difficult to estimate a fracture frequency valid for the entire borehole. The weighted sum for each of the three sections was calculated separately. The weighted sums for the upper- and lowermost sections were then multiplied by 1.25 in order to compensate for the lacking number of methods. The three sections were then put together and the power function from KSH01A was applied. Thus, the achieved estimated fracture frequency is a bit rough and should be taken with care.

4. Report evaluating the results (this report).

Table 4-3. Threshold values and weights used for estimating position of fractures and calculate estimated fracture frequency, respectively.

	Borehole	Sonic	Focused res. 300	Caliper	SPR	Normal res. 64	Lateral res.
Threshold	KSH02/KAV01	0.4/no data	0.4/no data	0.15/0.5	no data/1.0	no data/2.7	no data/1.2
Weight	KSH02/KAV01	2.5/no data	2.3/no data	3.3/3.3	no data/1.3	no data/0.55	no data/0.8

4.4 Data handling

The delivered data have been inserted in the database (SICADA) of SKB. The SICADA reference to the present activity is Field Note No. 292.

5 Results

5.1 Compilation and interpretation of petrophysical data

The sampling covers 21 samples from KSH02 and 15 from KAV01. Two of the samples from KAV01 (depths 45.495 m and 48.500 m) were collected at a late stage of the project only to investigate a questionable gamma-gamma anomaly. Only wet density was measured on these two samples, thus in the general compilation of data from KAV01 only 13 samples are included.

Each rock type group conforms to the SKB standard and the classification follows the core logging (Boremap) classification.

5.1.1 Petrophysical properties of KSH02

For KSH02 special emphasis was put on evaluating how plastic deformation and alteration affects the physical properties of the fine-grained dioritoid rock that dominates the bedrock of the Simpevarp peninsula. Nine samples were therefore collected from sections with primary fine-grained dioritoid, three from sections where the rock type is plastically deformed and six samples from section where the rock has suffered from intense alteration. The remaining three samples are classified as fine-grained mafic rock (or fine-grained diorite to gabbro).

The rock type classifications diagram in Figure 5-1 shows the distribution of the magnetic susceptibility versus density for each sample group. All nine primary fine-grained dioritoid samples plot on, or close to, the tonalite rock type curve. Their average wet density is 2780±17 kg/m^3 and the average magnetic susceptibility is 0.025±0.015 SI. The average density of the three plastically deformed samples is 2793±3 kg/m^3, which completely overlaps that of the primary samples. However, the lower average susceptibility of the deformed samples, Kmean = 0.012 SI (only 3 samples), may indicate that the deformation has affected the magnetization. The average density of the strongly altered samples is 2717±29 kg/m^3, which is significantly lower than for the primary as well as for the deformed rock samples. The average susceptibility of Kmean = 0.0021±0.0018 SI is also clearly lower than for the primary samples. The alteration appears to have destroyed most of the magnetite of this rock.

The three fine-grained mafic rock samples (or fine-grained diorite to gabbro) cluster fairly well in the middle of the tonalite and diorite rock type curves. Their average density is 2851±10 kg/m^3 and their average mean susceptibility is Kmean = 0.069±0.011 SI.

It must be noted that the rock types used in the rock classification diagram do not conform perfectly to the geology of the Simpevarp area. There is for example no corresponding rock type curve for fine-grained dioritoid, a rock type that occurs frequently in the area. This misfit is caused by the lack of high quality average density data and corresponding petrology data for these rock types. We therefore suggest that the data in rock classification diagram such as shown in Figure 5-1 should be used as indicators of the compositional variation between different rock types (or groups of rocks), and that these diagrams will be used to help identifying possible faulty rock classifications during the geological core logging and also to spot geographical variations in rock composition.

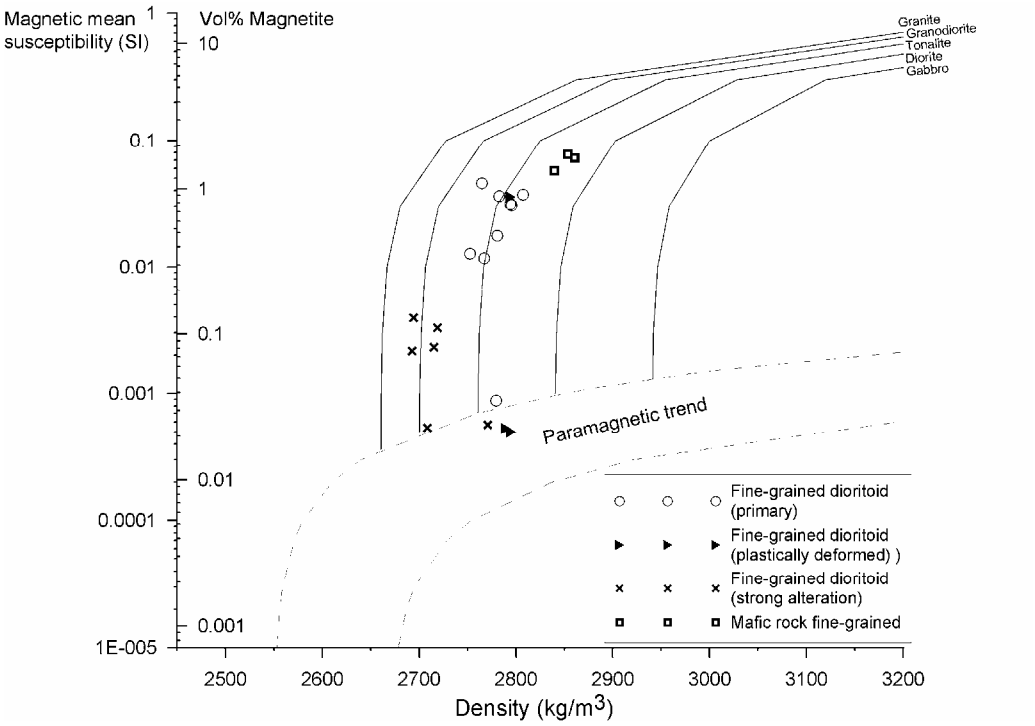

Figure 5-1. *Density-susceptibility rock classification diagram for rock samples in KSH02. See the text for explanation.*

Q-values (Figure 5-2) average at Q = 0.28 and the distribution of the data is narrow, which is indicated by the low standard deviation of 0.13. Neither alteration nor plastic deformation seems to affect the Q-values, but clearly lowers the NRM intensity of the fine-grained dioritoid. This result indicates that plastic deformation or alteration decreases the amount of ferromagnetic minerals, but it does not alter the composition of the magnetic mineralogy.

In Figure 5-3 the porosity is plotted against magnetic susceptibility. There is a significantly higher porosity and lower susceptibility for the altered fine-grained dioritoid samples compared to the primary samples. However, with respect to the low number of samples, it appears as if plastic deformation destroys the magnetic minerals but do not affect the porosity.

As stated in section 4-1 it is possible to interpret the inclination of the remanence vector, the inclination of the magnetic lineation and the dip of the magnetic foliation plane with an accuracy of ca ±5°. In Figure 5-4a the NRM inclination versus depth is shown. A majority of the samples show positive inclinations of ca. 40°–70°. Two samples have negative inclination. The magnetic lineation (Figure 5-4b) is generally shallow dipping, below 20° for a majority of the samples and the magnetic foliation planes (Figure 5-4c) display moderate to steep dips at 0–700 m depth and shallow dips below 700 m depth. The degree of anisotropy shows a clear correlation to the magnetic susceptibility and can therefore not be used as an indicator of the degree of tectonic strain.

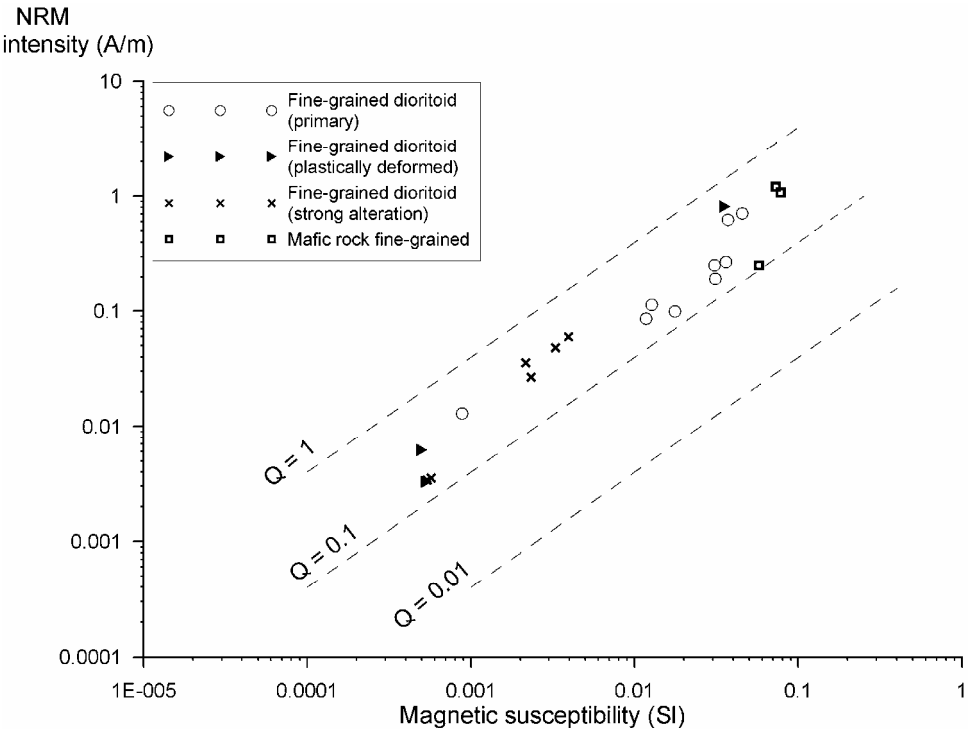

Figure 5-2. *NRM intensity versus magnetic susceptibility for rock samples in KSH02. Hatched lines indicate Q-values of 0.01, 0.1 and 1. See the text for explanation.*

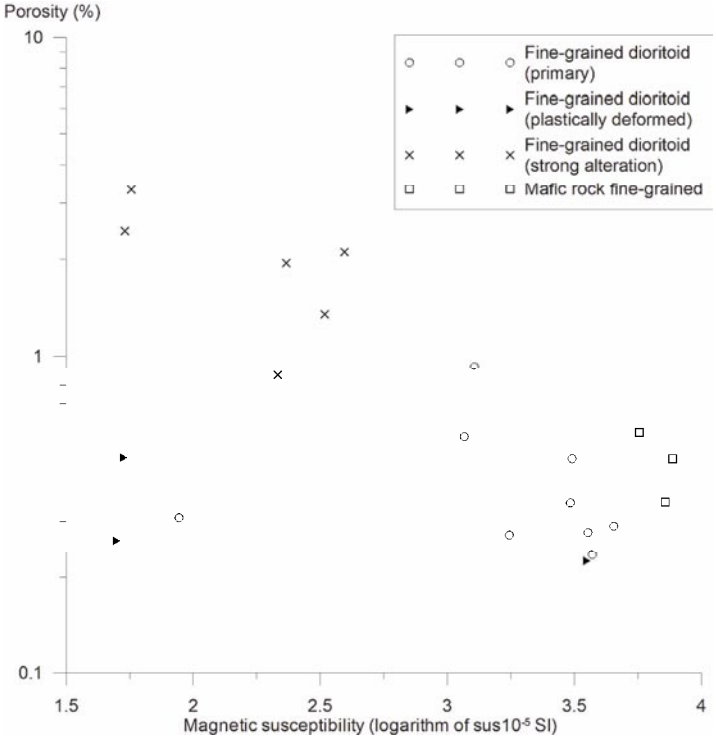

Figure 5-3. *Porosity versus magnetic susceptibility for rock samples in KSH02. See the text for explanation.*

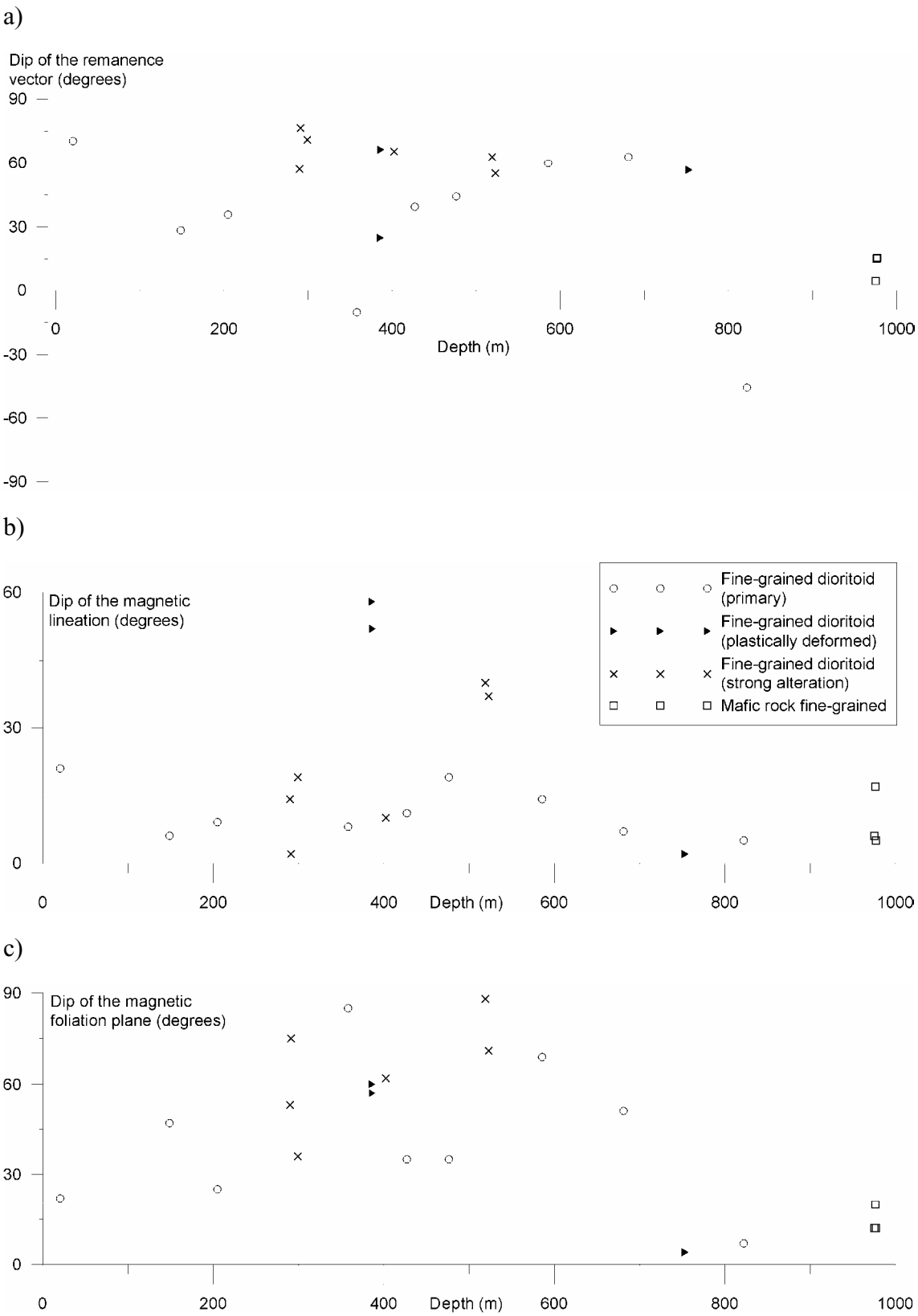

Figure 5-4. *a) NRM inclination versus depth for rock samples in KSH02, b) inclination of the magnetic lineation versus depth and c) dip of the magnetic foliation plane versus depth. See the text for explanation.*

The rock samples in this study are not expected to contain any minerals that contribute significantly to the bulk electrical conductivity of the rock. The electric resistivity is therefore dependent upon electrolytic conduction in water-filled pore space. The relation between electric conductivity (inverse of resistivity) and porosity can be estimated with the empirical Archie's law (assuming water saturated samples):

$$\sigma = a \cdot \sigma_w \cdot \varphi^m \qquad (5\text{-}1)$$

where

σ = bulk electrical conductivity (= $1/\rho$, electric resistivity)
σ_w = electric conductivity of pore water
f = pore volume fraction of sample
a = constant that accounts for surface conductivity (see below)
m = constant that accounts for pore space geometry

Archie's law has been proven to work well for sedimentary rocks with high porosity. Good fits of experimental data for crystalline rocks are not often seen but the formula can still serve as a model that helps understand how the electrical properties of crystalline rocks relates to pore space structure. The factor *a* in Equation 5-1 accounts for the so called surface conductivity that is schematically illustrated in Figure 5-5. The effective conductivity of the pore water is increased close to the surface of mineral grains due to the formation of an electric double layer of ions in the electrolyte. This will have little effect if the pores are very wide and/or filled with saline water but may be very significant for thin pores and fresh water conditions. Rocks that contain significant amounts of e.g. chlorite, fine-grained mica or clay minerals are thus expected to show high values for the parameter *a* (Figure 5-6). Note that Equation 5-1 is written slightly different than Archie's law in section 4.3 where an extra constant was introduced to explain surface conductivity.

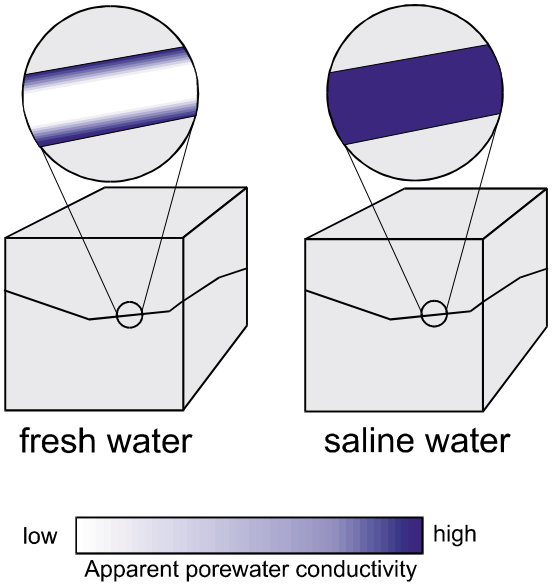

Figure 5-5. *An electric double layer at the interface between pore water and mineral grains will locally increase the effective electric conductivity of the water. The conductivity of the unaffected fresh water is illustrated by white colour in the left part of the figure. The effect will more or less vanish in saline water (right).*

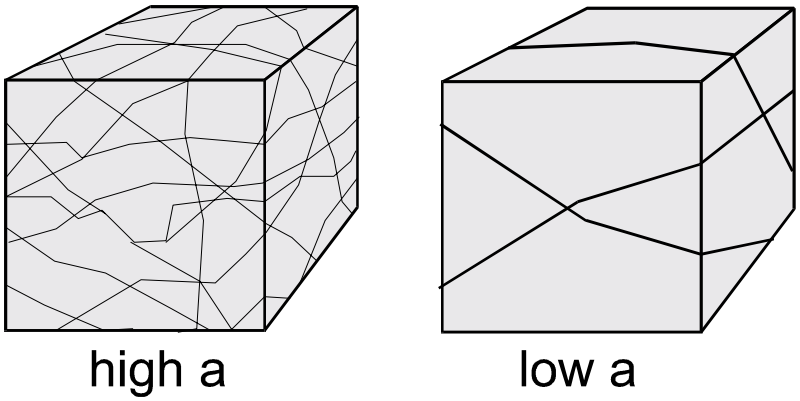

Figure 5-6. *The rock sample in the left part of the figure contains a lot of thin pore spaces and will thus apparently show a high value for the parameter a in Archie's law. The sample to the right, with wider pore spaces, might have the same porosity but will be less affected by surface conductivity. The resistivity of this sample will therefore be higher and the apparent a-value will be lower.*

The parameter *m* in Archie's law accounts for pore space geometry. It will have the value 1 for straight pores with constant cross-sectional area. High values for *m* indicates that the pore volume has a geometry that is unfavourable for electric current conduction. This will happen if the current paths are crocked and if the pore space contains constrictions, vugs and "dead-ends" (Figure 5-7).

In general it is not possible to estimate the values of *a* and *m* separately from measurements of porosity and resistivity. However, since surface conduction effects become less significant in saline environments it is possible to get a reasonable estimate of *m* from the measurements made on samples soaked in saline water:

$$m = \ln(\varphi)/[\ln(\sigma) - \ln(a \cdot \sigma_w)] \qquad (5\text{-}2)$$

Figure 5-8 shows a plot of resistivity in saline water versus porosity. Straight lines corresponding to different values of *m* are also plotted. Surface conduction effects will not vanish completely in water with the salinity used in this study. A reasonable value of *a* has therefore been assumed in the plot. This value was set to 4.0.

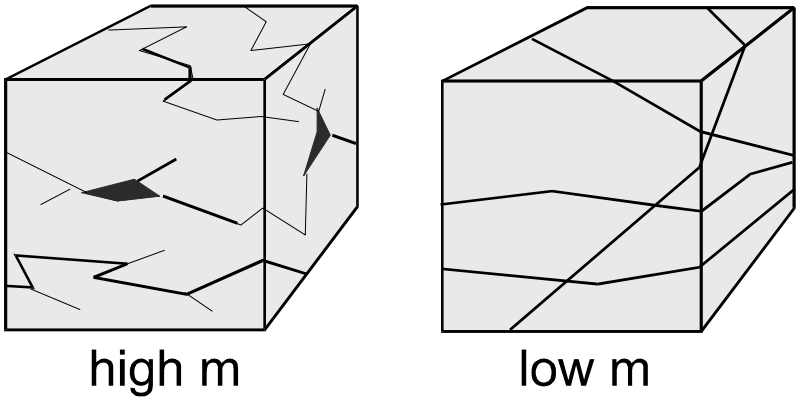

Figure 5-7. *The rock sample in the left part of the figure contains pore space with constrictions, vugs and "dead-ends". In combination with crocked current paths this will give a high apparent value of m in Archie's law. Straight current paths with constant cross-sectional area, as in the right example, will give a low apparent m-value.*

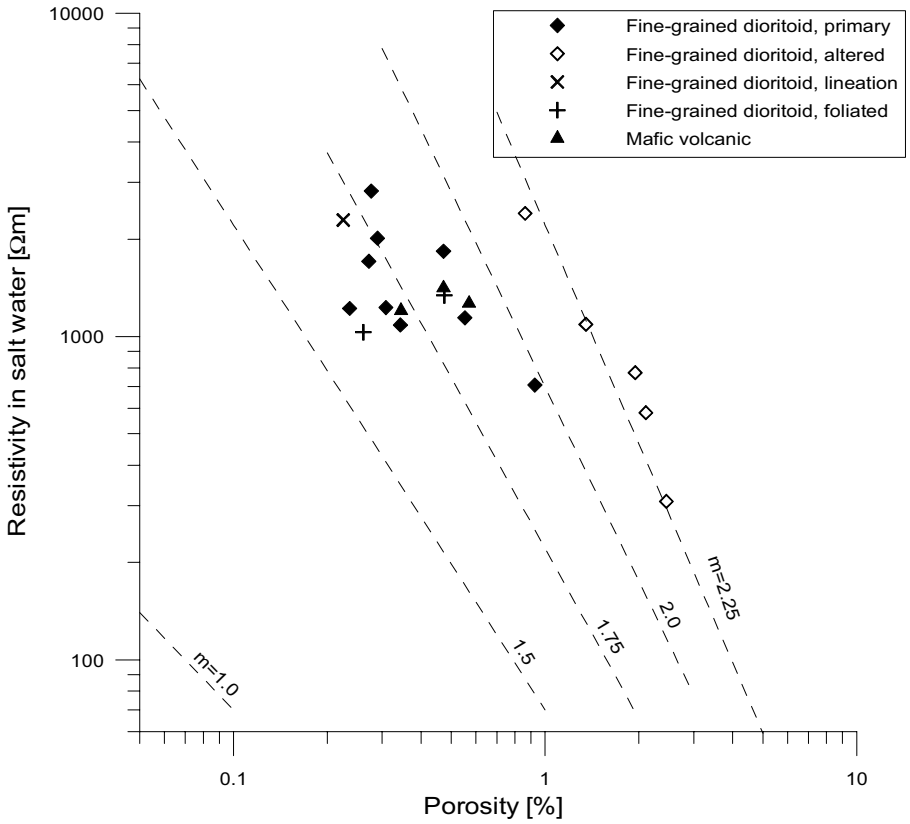

Figure 5-8. *Resistivity in saine water versus porosity for rock samples in KSH02. The dashed lines corresponds to resistivities calculated with Archie's law for different values of the parameter m and with a=4.0.*

The strongly altered samples all have high porosity and also show high apparent *m*-values of around 2.25. The other samples show lower apparent *m*-values (1.6 to 2.0) and lower porosities. The resistivity of the altered samples is in general lower than the other samples although there is an overlap.

The resistivity measured in fresh water as a function of porosity can be seen in Figure 5-9. The altered samples have lower resistivities (geometric mean 3635 Ωm) than the other samples (geometric mean 24365 Ωm). The variation is however quite large (standard deviation 0.42 and 0.35 decades respectively). Straight lines corresponding to different values of *a* in Archie's law have also been included in Figure 5-9. A value of 1.75 for *m* has been assumed for these lines. This means that the lines are not valid for the altered samples. Most of the samples not belonging to the altered group show apparent *a*-values ranging from 10 to 30. This means that surface conduction dominates over simple electrolytic conduction and that pore space area and not volume will determine the resistivity of samples in fresh water.

Combining Equations 5-1 and 5-2 and rearranging yields an expression for apparent values of the parameter *a*:

$$a = \sigma_f/\sigma_{wf} \cdot (a_s \cdot \sigma_{ws}/\sigma_s) \qquad (5\text{-}3)$$

where the subscripts f and s stands for measurements in fresh and saline water respectively. The apparent values for *a* and *m* are plotted against each other in Figure 5-10. The altered samples group in the upper right part of the graph with high values for both parameters.

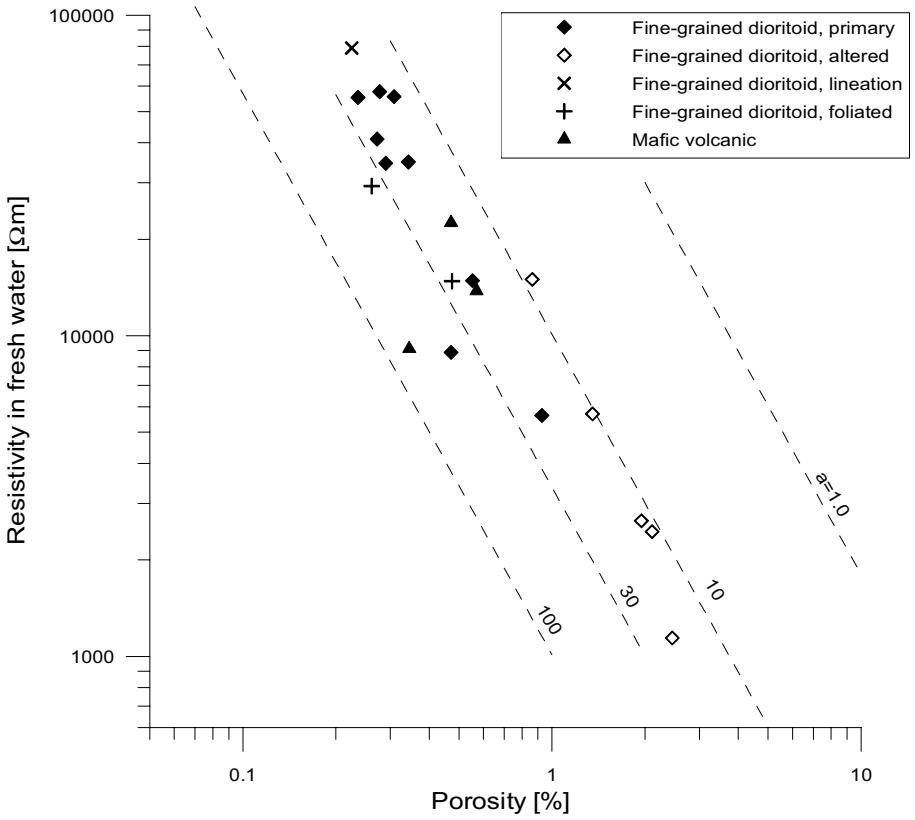

Figure 5-9. *Resistivity in fresh water versus porosity for rock samples in KSH02. The dashed lines corresponds to resistivities calculated with Archie's law for different values of the parameter a and with m=1.75.*

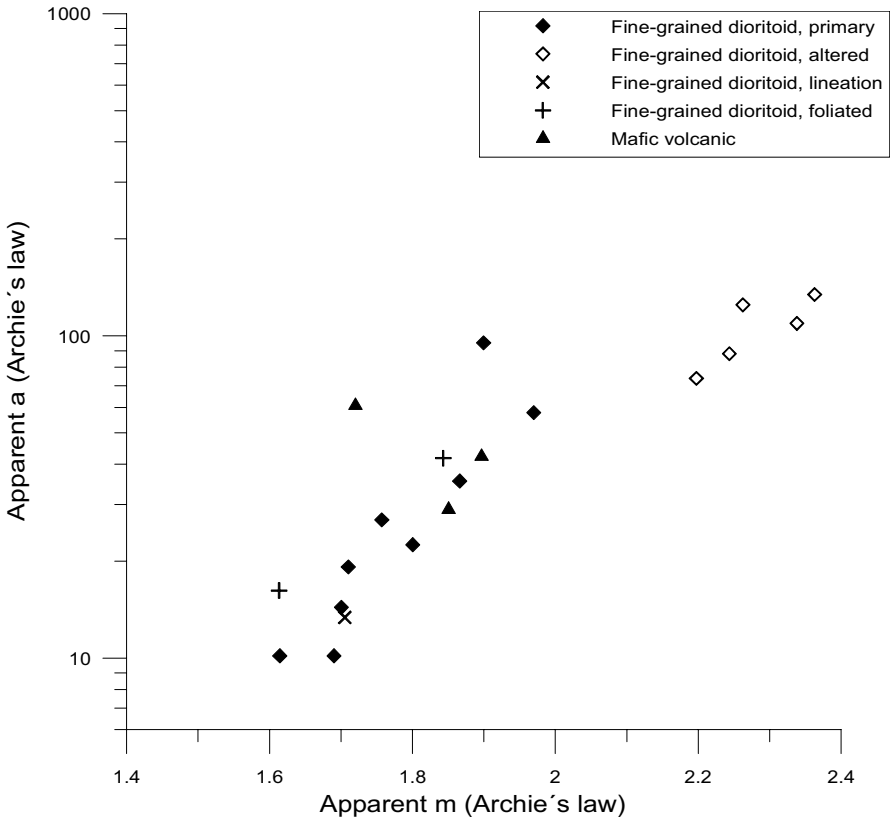

Figure 5-10. *Apparent values of a and m in Archie's law for rock samples in KSH02.*

The rest of the samples also show a trend that might correspond to alteration. The primary dioritoid samples that have been commented as “weak alteration” in Table 4-1 plot at the centre of the graph whereas fresh samples plot at the lower left part of the graph.

The induced polarization (expressed as phase angle between injected current and observed potential difference) in fresh and saline water is plotted in Figure 5-11. The values are generally low and quite normal for non-mineralized crystalline rock. The mean is 10.1 mrad with a standard deviation of 3.1 mrad for the fresh water measurements. The mafic rock samples have higher values (mean 13.4 mrad, standard deviation 0.8 mrad) compared to e.g. the primary dioritoid (mean 8.9 mrad, standard deviation 3.3 mrad). The phase angles decreases to very low values in saline water for most samples. This indicates that membrane polarization is the dominating polarization mechanism. The altered samples do however show some polarization in saline water. This indicates a presence of minerals with electronic conduction in these samples.

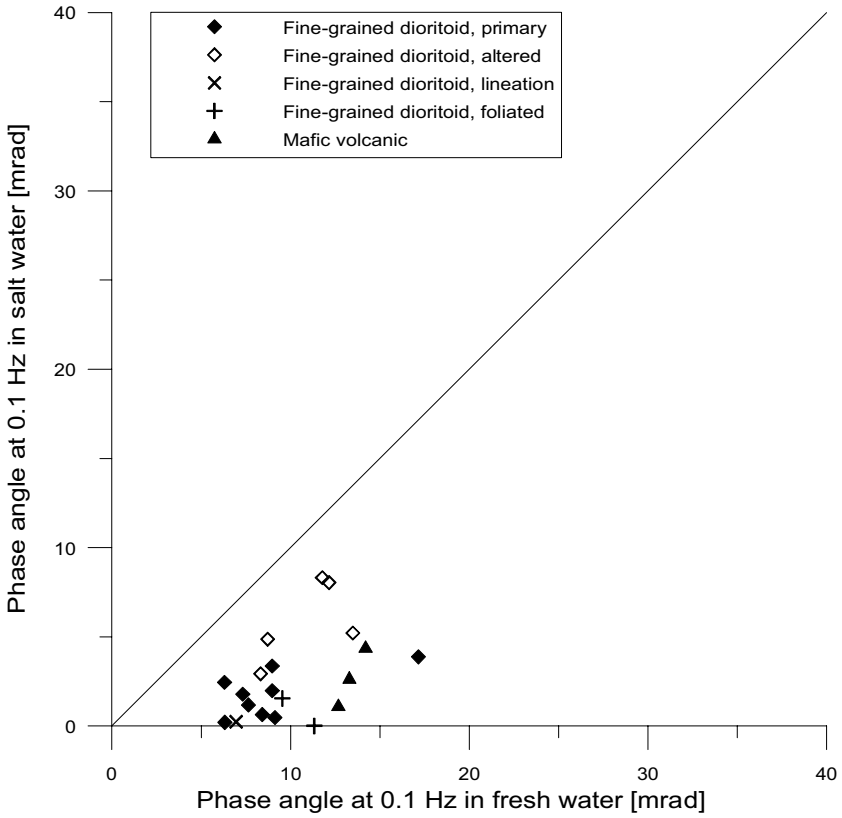

Figure 5-11. *Induced polarization in fresh and saine water for rock samples in KSH02.*

5.1.2 Petrophysical properties of KAV01

The sampling of the core of KAV01 includes 7 samples classified as Ävrö granite and 6 samples preliminary classified as fine-grained dioritoid (plus the two extra Ävrö granite samples mentioned in section 5.1 above. Those two are not included in the following chapter). The "fine-grained dioritoid" samples clearly differ in appearance from each other. Three of them look like fine-grained mafic rock (depth co-ordinates 16.58 m, 78.08 m and 650.9 m); two remind a great deal of fine-grained dioritoid (depth co-ordinates 364.08 m and 610.08 m) and one sample looks more like granite to granodiorite rock (depth co-ordinate 170.13 m). The rock classification diagram (Figure 5-12 below) displays the magnetic susceptibility versus wet density for the samples from KAV01. The Ävrö granite samples cluster tightly close to the granite curve. The average density of the Ävrö granite is 2680±8 kg/m^3 and the average mean susceptibility is 0.020±0.004 SI. The other samples scatter widely in density, from 2713 kg/m^3 to 2923 kg/m^3, and also in magnetic susceptibility, from 0.0005 SI to 0.0487 SI, which may indicate that they belong to different rock type groups.

The Q-values (Figure 5-13) of the Ävrö granite vary from Q = 0.03 to Q = 0.54, with an average of Q = 0.28. The other samples have a narrower distribution and an average of Q = 0.16. Two of the "dioritoid samples" that look like mafic volcanite have significantly lower NRM intensity and magnetic susceptibility then the majority of the samples, which may indicate alteration. The dip of the remanence vector is positive and moderate or steep for all the measured samples. No significant variations with depth are seen.

The average degree of magnetic anisotropy is P = 1.21 for the Ävrö granite rock samples and P = 1.19 for the other samples, which are normal values for primary igneous rocks.

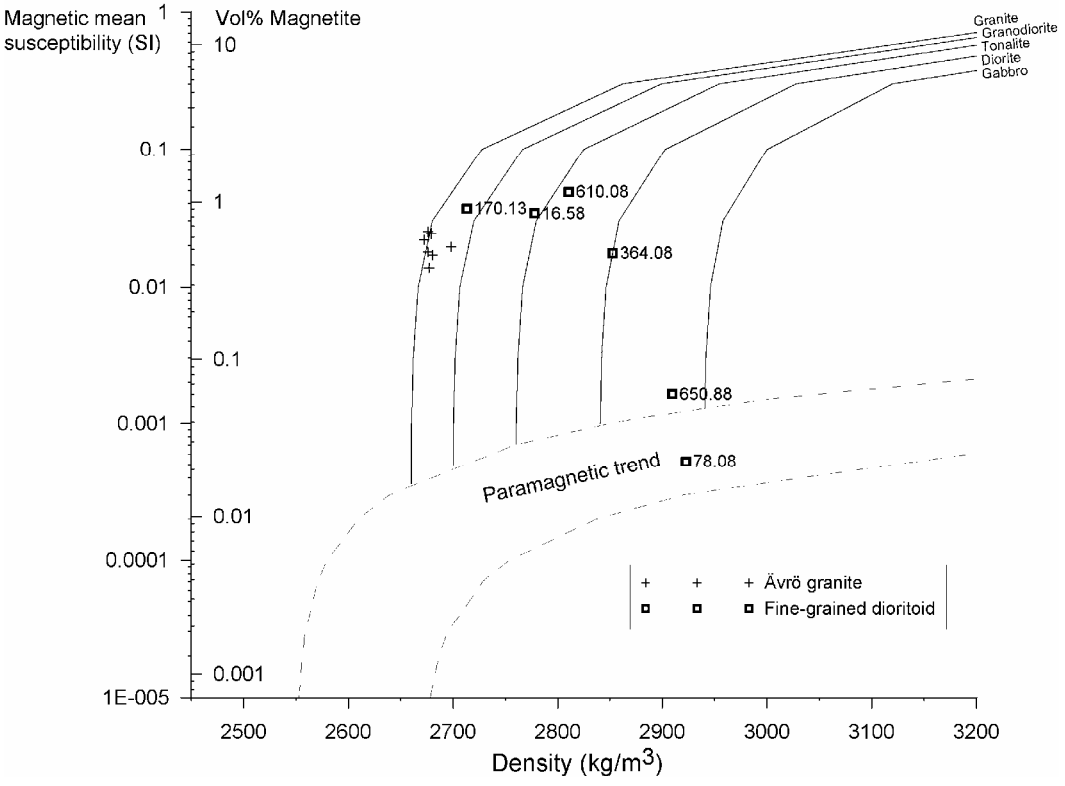

Figure 5-12. *Density-susceptibility rock classification diagram for rock samples in KAV01. The numbers attached to the fine-grained dioritoid sample symbols display the depth co-ordinate of each sample respectively. See the text for explanation.*

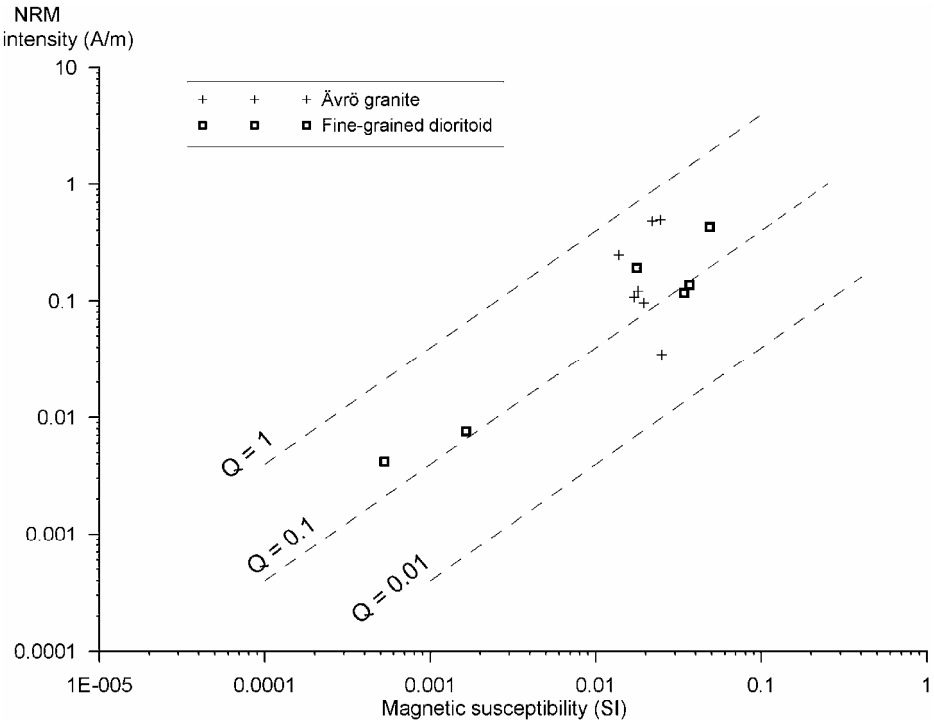

Figure 5-13. *NRM intensity versus magnetic susceptibility for rock samples in KAV01. Hatched lines indicate Q-values of 0.01, 0.1 and 1. See the text for explanation.*

The dip of the magnetic lineation averages at ca. 30° and the average dip of the magnetic foliation planes is ca. 50°. No significant variations with depth are seen in the AMS data.

The electric resistivity in fresh water versus porosity can be seen in Figure 5-14. The dioritoid samples have very low porosity and also very high resistivity. The granite samples have fairly normal resistivity and porosity values. The geometric mean of the resistivity is 11290 Ωm for the granite samples and 35370 Ωm for the dioritoid samples. The standard deviations are 0.12 and 0.39 decades respectively. The values for the dioritoid samples are similar to those seen for primary dioritoid samples in KSH02.

Apparent a- and m-values have been calculated according to the equations (5-2) and (5-3). The results are shown in Figure 5-15. The samples plot along a similar trend as the KSH02-samples in Figure 5-10. There are however no samples in Figure 5-15 corresponding to the altered samples in Figure 5-10. All dioritoid samples except one plots in the “fresh rock” corner of the graph. The granite samples show higher a- and m-values indicating that there might be a systematic difference in pore space geometry between the rock types.

The induced polarization data in fresh and saline water can be seen in Figure 5-16. Both rock types have low and fairly normal values in fresh water. All dioritoid samples except one have low IP values in saline water indicating that membrane polarization is the dominating mechanism. The anomalous sample is the same one that shows high apparent a- and m-values in Figure 5-15. Visually, that sample does however not appear to be more altered than the other samples. The granite samples show some residual IP effect in saline water indicating presence of minerals with electronic conduction. No significant correlation between IP in saline water and magnetic susceptibility can be seen so magnetite is not likely to be the cause of the IP.

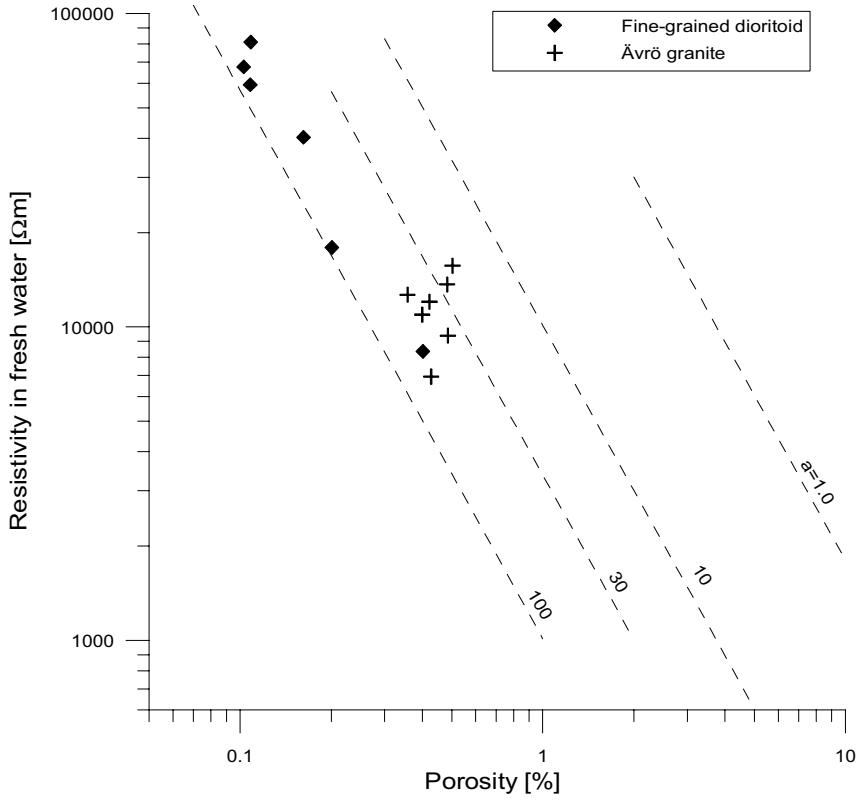

Figure 5-14. *Resistivity in fresh water versus porosity for rock samples in KAV01. The dashed lines correspond to resistivities calculated with Archie's law for different values of the parameter a and with m=1.75.*

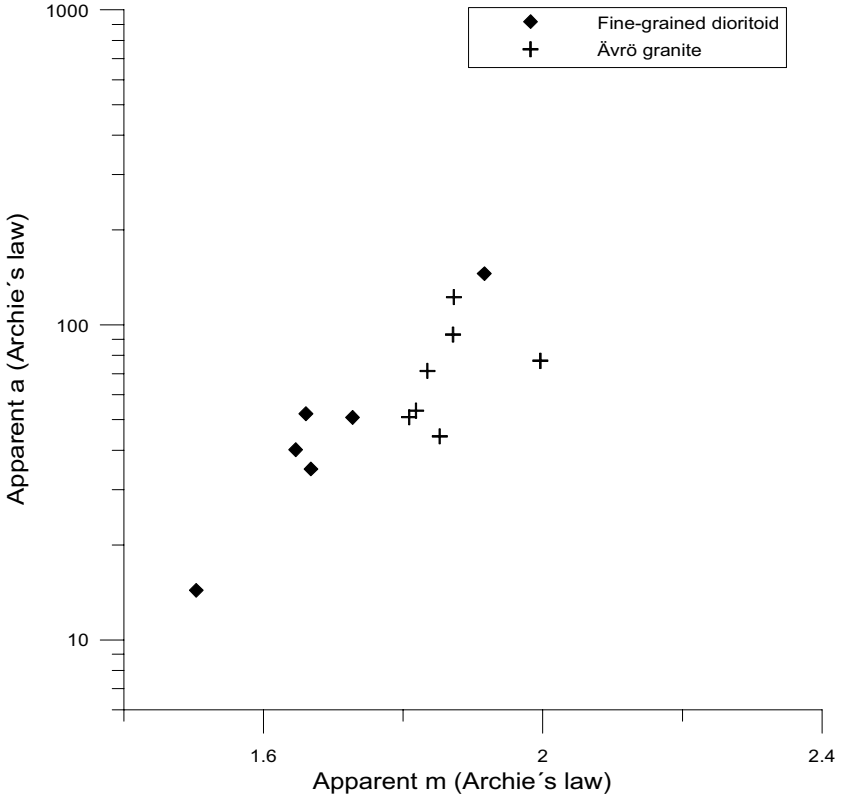

Figure 5-15. *Apparent values of a and m in Archie's law for rock samples in KAV01.*

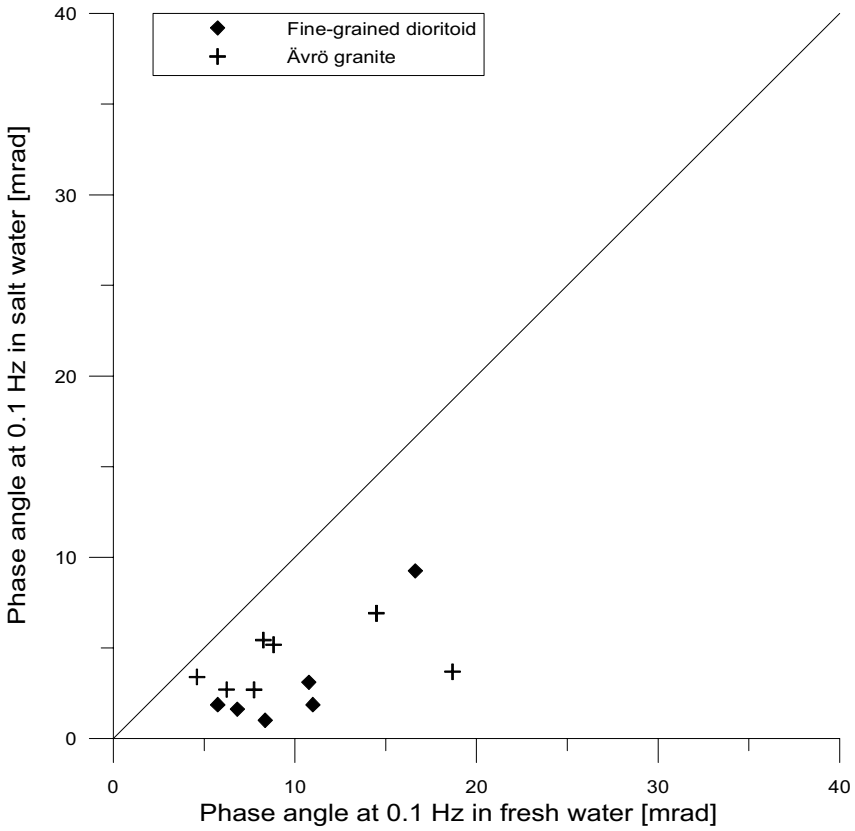

Figure 5-16. *Induced polarization in fresh and saine water for rock samples in KAV01.*

Values for *a* and *m* in Archie's law are needed to calculate apparent porosity values from resistivity logs. It is not possible to use the average values from the data seen in Figure 5-15 since the actual borehole fluid resistivity is intermediate between the resistivity of the fresh and saline water resistivity measurements on the samples. The parameters were estimated through a non-linear interpolation between fresh water and saline water data. The results are presented in Table 5-1.

Table 5-1. Values of the constants *a* and *m* in Archie's law used in the calculation of the apparent porosity for KAV01.

Borehole	Average fluid resistivity (Ωm)	a	m
KAV01	19	10.5	31.662

5.2 Control of the logging data

5.2.1 Noise levels and qualitative control

Noise levels of the raw data for each logging method are presented in Table 5-2 below. The top 70 m of KAV01 were disregarded in the calculation of the noise levels. Noise levels are only presented for the data used in the interpretation. For a majority of the logging data (except density and sonic) the noise is lower, or only slightly higher, than the recommended level. All logging data were filtered prior to the interpretation.

A qualitative inspection was performed on the loggings. The data were checked for spikes and/or other obvious incorrect data points. Such erroneous data points were discovered in the sonic logging of KSH02 at 31 sections (usually 1–2 data points) and were replaced by values interpolated from surrounding data. The inspection also indicates that the caliper logging data of the uppermost 70 m of KAV01 are very noisy and these data are therefore not included in the interpretation of fractures.

During the length adjustment operations in KAV01 a level difference was noted between the natural gamma radiation logging from 1986 (Malå GeoScience) and the one from 2003 by Rambøll. The mean level of the 2003 data is approximately 5 µR/h higher than for the 1986 data. There are also differences between the fluid temperature and the fluid resistivity data from 1986 and 2003. In the fluid resistivity data from 1986 there is a very sharp step wise decrease in resistivity at ca 560 m depth, which clearly looks like a probable boundary between lesser and more saline water. In the 2003 data there is instead a smooth and symmetric minima centered at ca 650 m depth. We assume that the 1986 data indicate more stable conditions and these data were therefore used to estimate the borehole fluid salinity (the 1986 data were of course also used in the correction of the 1986 normal resistivity logging). However, the 2003 fluid temperature data were used for calculating the vertical fluid temperature gradient, since these data have 10 times higher resolution and also appear to be less noisy than the 1986 data.

Table 5-2. Noise levels in geophysical logging data for KSH02 and KAV01.

Logging method	KSH02	KAV01	Recommended max noise level
Density (kg/m^3)	21	17	3–5
Magnetic susceptibility (SI)	2×10^{-4}	1×10^{-4}	1×10^{-4}
Natural gamma radiation (µR/h)	0.6	1.9	0.3
Lateral resistivity (%)	No data	1.7	2.0
Short normal resistivity (%)	No data	No data	2.0
Long normal resistivity (N64) (%)	No data	0.5	2.0
Single point resistance (%)	No data	0.6	No data
Fluid resistivity (%)	0.07	1.7	2.0
Fluid temperature (°C)	0.0002	0.02	0.01
Caliper (meter)	0.00002	0.00004	0.0005
Focused resistivity 300 (%)	21	No data	No data
Focused resistivity 140 (%)	4	No data	No data
Sonic (m/s)	42	No data	20

5.2.2 Comparsion between logging and petrophysical data for KSH02

A quality control of the gamma-gamma and the magnetic susceptibility loggings is performed by comparing the logging data to the petrophysical data at the corresponding depths. In Figure 5-17 the gamma-gamma (density) logging is plotted versus wet density sample measurements. The correlation is very good and the slope of the fitted line of 1.004 (fit through origin) indicates that the density level of the logging tool corresponds well to the sample measurements. There is some scatter in the data and the residual root mean square value, which indicates the accuracy of the logging density, is 60 kg/m^3. However, the plot in Figure 5-17 shows raw data, and for the interpretation we use filtered data. The filtering procedure reduces the scatter significantly.

A similar plot between the susceptibility logging and susceptibility measured on core samples is shown in Figure 5-18. There is an excellent correlation between logging and petrophysical data, however the slope of the fitted line (through origin) is 0.497, which indicates that the logging measurements underestimate the true magnetic susceptibility. Also note that there is a slight misfit between the fitted line and the data. Trying to improve the correction of the logging data a linear fit was therefore also tested (the hatched curve). However, the fit through origin is considered better than the linear fit. Prior to the interpretation the logging data were corrected by use of the equation from the fit through origin.

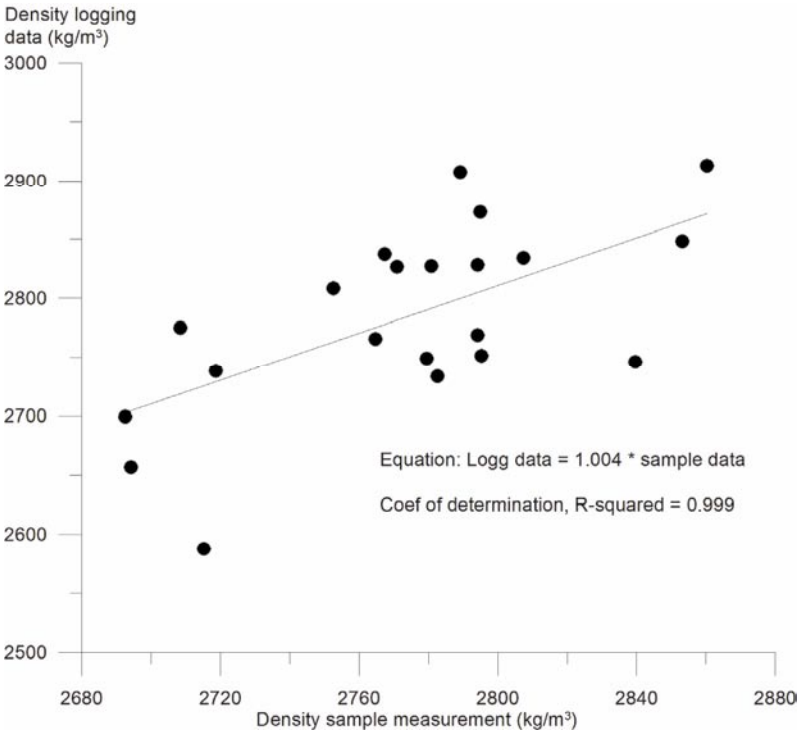

Figure 5-17. *Cross plot of density logging data versus density data for rock samples from KSH02.*

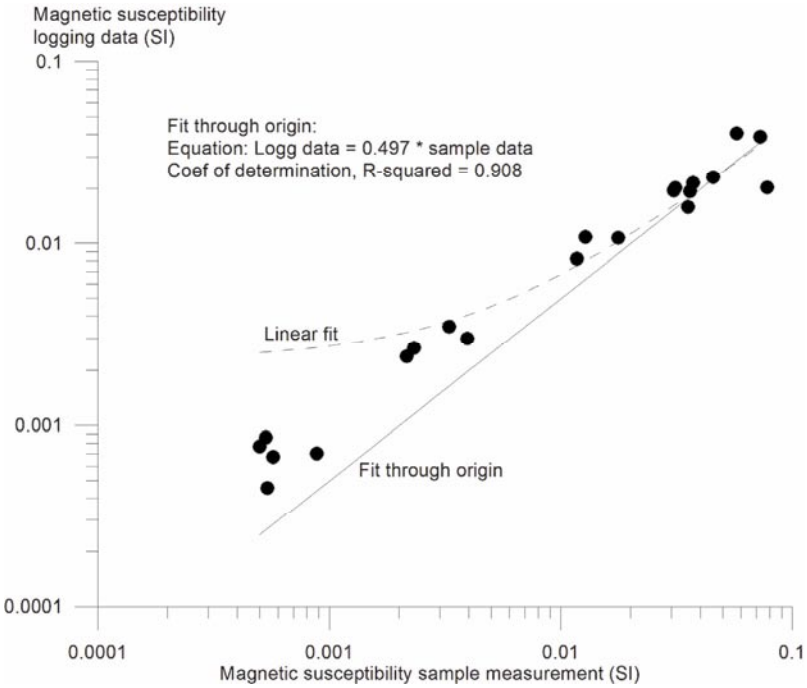

Figure 5-18. *Cross plot of magnetic susceptibility logging data versus susceptibility data for rock samples from KSH02.*

5.2.3 Comparsion between logging and petrophysical data for KAV01

The quality control of the gamma-gamma and the magnetic susceptibility loggings is performed by comparing the logging data to the petrophysical data at the corresponding depths. For KAV01 this control was performed separately for the top 70 m, for which the diameter is significantly larger than for the rest of the borehole. In Figure 5-19a the gamma-gamma (density) logging is plotted versus wet density sample measurements for the top 70 m. Two of the data points come from a density anomaly at ca 44–50 m depth (see the diagram) where the logging data indicate densities of ca 3000 kg/m^3, which correspond to diorite to gabbro rocks. However, the section is classified as Ävrö granite. The two sample measurements both indicate a density of ca 2670 kg/m^3, which suggests that the logging data are erroneous. We therefore suggest that the density logging data along the entire section 44–50 m should be disregarded. Comparing the logging and petrophysical data for the remaining two points suggests that the density logging underestimates the true density by ca 10%. The logging data were corrected for this prior to the interpretation. In Figure 5-19b logging and sample densities are shown for the section 70–745 m. As seen in the figure the correlation between logging and petrophysical data is fair, even though the number of data points is few and the data distribution is unsuitable for statistical evaluation. Fits to the data indicate that the density logging overestimates the true density by ca 10%. The logging data were corrected for this prior to the interpretation.

Diagrams comparing the susceptibility logging data to petrophysical measurements are shown in Figure 5-20. In Figure 5-20a we see the two data points for the top 70 m of the borehole. Comparing the logging and petrophysical data for the two points suggests that the susceptibility logging underestimates the true magnetic susceptibility by ca 60%. The logging data were corrected for this prior to the interpretation. In Figure 5-20b the section 70–745 m is shown. Comparing the logging and petrophysical data shows a very good correlation. By use of a fit through the origin there is an indication that the susceptibility logging underestimates the true magnetic susceptibility by ca 60% (the same value as reported for the top 70 m). The logging data were corrected for this prior to the interpretation.

a)

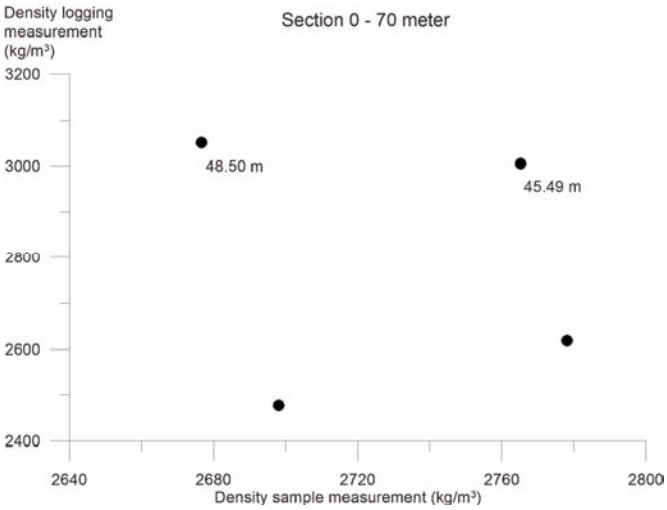

b)

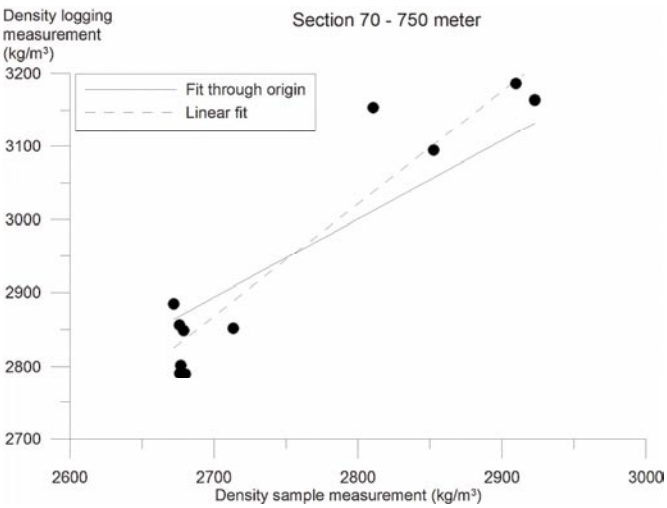

Figure 5-19. *Cross plot of density logging data versus density data for rock samples from KAV01 for a) section 0–70 m and b) section 70–750 m.*

a)

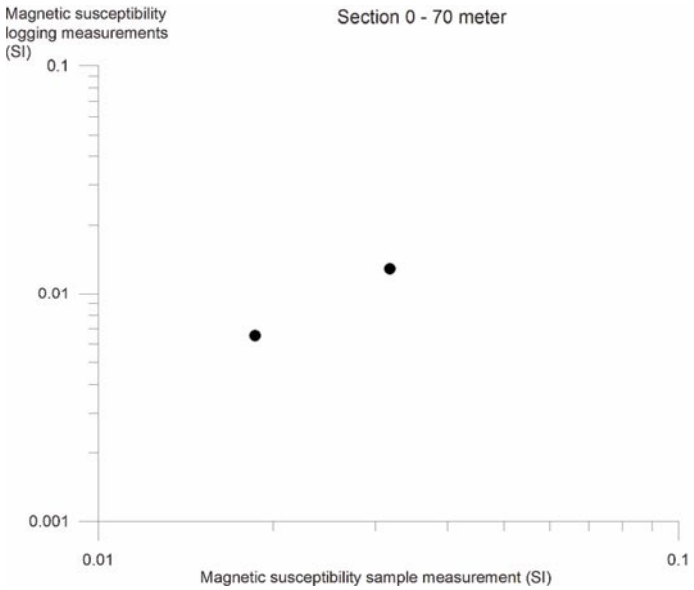

b)

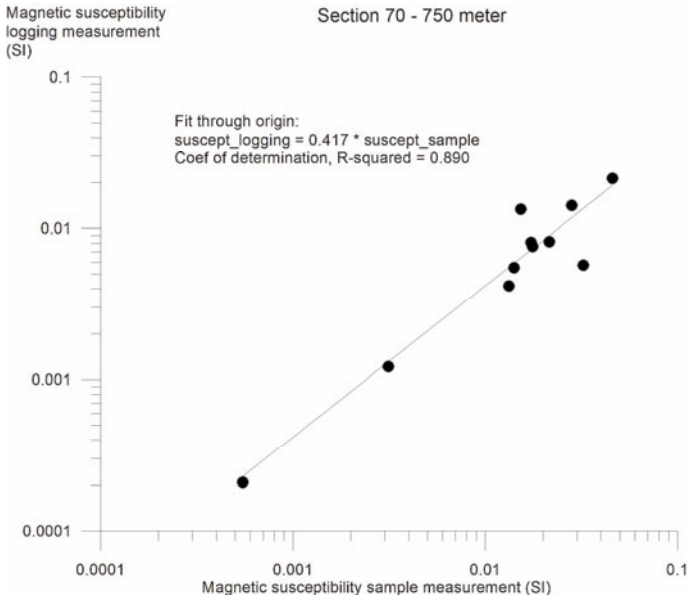

Figure 5-20. *Cross plot of magnetic susceptibility logging data versus magnetic susceptibility data for rock samples from KAV01 for a) section 0–70 m and b) section 70–750 m.*

5.3 Interpretation of the logging data

A complete presentation of all processed loggings and interpretation products is given in Appendices 1 and 2.

5.3.1 Interpretation of KSH02

The results of the generalized data, possible alteration and fracture estimations together with geophysical logging data, salinity and vertical temperature gradient logs for the borehole KSH02 are presented in Appendix 1.

Correction of resistivity loggings and apparent porosity

No data to correct.

Vertical temperature gradient and salinity

The average vertical temperature gradient in KSH02 is 13.9°C/km. A few minor anomalies are seen at depths ca 170 m, 400–420 m, 530 m and 740 m; and two prominent anomalies are seen at ca 100 m and 855 m depth (Figure 5-21). The former coincides with a large low resistivity and low P-wave velocity zone and the latter can possibly be related to an increase in the water salinity that starts at ca 820 m depth (Figure 5-21).

The estimated salinity is close to 0 ppm NaCl the for the uppermost 200 m. Between 200 m and 400 m depth it increases to ca 16 000 ppm NaCl, where it lays stable down to ca 820 m depth where a second increase starts, continuing up to ca 40 000 ppm NaCl at 1000 m depth.

Interpretation of lithology and fractures

A majority of the rocks along the borehole have silicate densities indicating a mineral composition that corresponds to tonalite or diorite rocks. The natural gamma radiation generally varies between 20 µR/h and 30 µR/h. Between 500 m and 720 m depth there are several fairly long sections of “granite densities” and high gamma radiation, which is an indication of the occurrence of fine-grained granite. Rock alteration is indicated along the sections c. 360–400 m, 510–530 m and 890–900 m.

The estimated fracture frequency only indicates increased fracturing along the section c. 80–105 m and 730–745 m. However, when looking at the raw sonic and focused resistivity (300) data, there are also clear indications of low velocity and low resistivity zones along the sections 280–300 m, 515–525 m (which coincides with possible rock alteration, see above), and 555–580 m (which coincides with probable occurrence of fine-grained granite). It should be noted that the large temperature gradient anomaly at 855 m depth coincides with a major low resistivity anomaly, possibly indicating that there is a significant water bearing fracture at this depth.

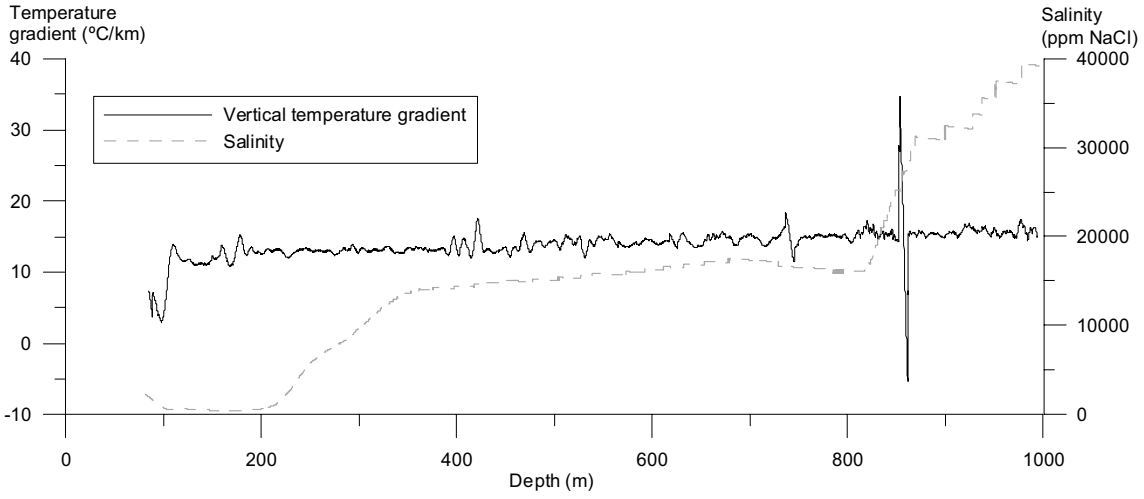

Figure 5-21. *Vertical temperature gradient and estimated salinity for KSH02.*

5.3.2 Interpretation of KAV01

The results of the generalized data, possible alteration and fracture estimations together with geophysical logging data, interpreted salinity, apparent porosity and vertical temperature gradient logs for the borehole KAV01 are presented in Appendix 2.

Correction of resistivity loggings and apparent porosity

The median resistivity of the uncorrected long normal resistivity logging is 18 kΩm, and after correction the median resistivity is 12 kΩm. The values correspond to "normal" unaltered crystalline rock. There are two major low resistivity anomalies, possibly related to fracture zones, at c. 430–450 m depth and 520–530 m depth.

An estimation of the apparent porosity, based on the long normal resistivity data, is presented in Figure 5-22. The calculation indicates that rock porosities are below 1% along most sections of the borehole, apart from two sections at ca 430–460 m and c. 520–560 m depth where the porosity is indicated at c. 1–2%.

Vertical temperature gradient and salinity

The vertical temperature gradient (based on the data measured by Rambøll in 2003) indicates a mean temperature gradient of ca 13.1°C/km. There are two large anomalies along the sections c. 420–465 m and 520–545 m (Figure 5-23). Both anomalies are thought to be related to increased fracturing of the bedrock.

The salinity (calculated on basis of data from 1986) varies between 200 ppm NaCl and 300 ppm NaCl along the uppermost 560 m of the borehole. At 560 m depth the salinity abruptly increases to c. 900 ppm NaCl and there is another increase at c. 640 m depth.

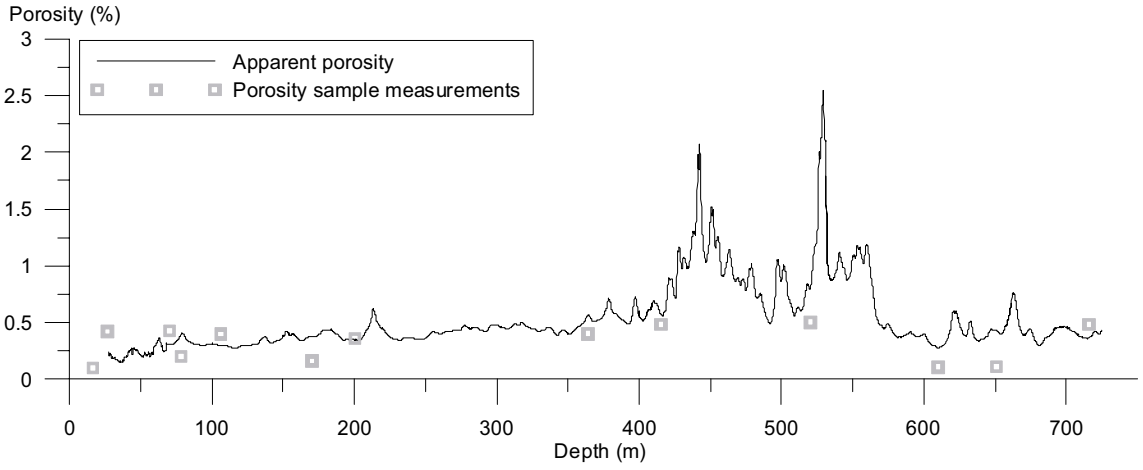

Figure 5-22. Full drawn line shows apparent porosity logging estimated from the long normal resistivity logging in KAV01. The squares indicate porosity data from sample measurements.

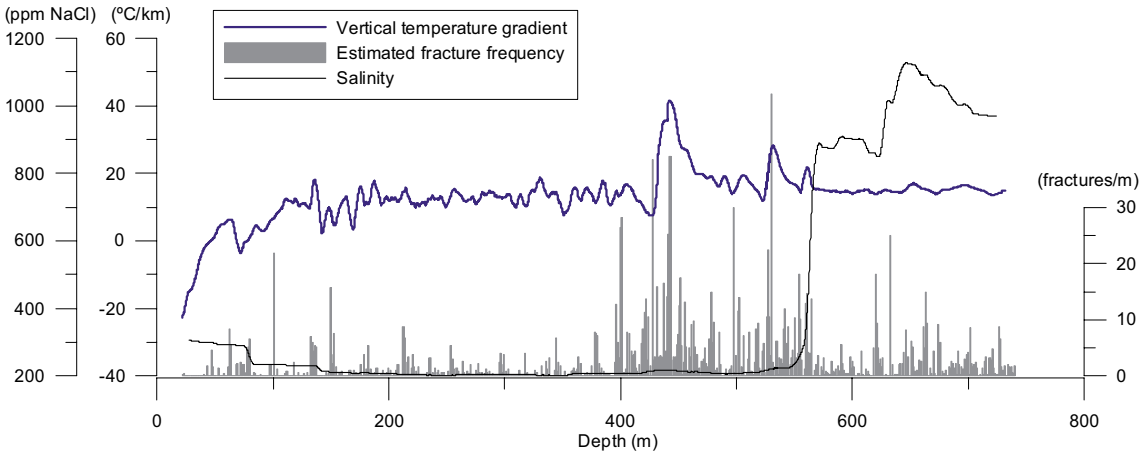

Figure 5-23. *Blue line shows vertical temperature gradient, black line shows estimated salinity and grey bars show estimated fracture frequency in KAV01.*

Interpretation of rock types and fractures

A majority of the rocks along the borehole have silicate densities indicating a mineral composition that corresponds to granite and granodiorite rocks. The uppermost 130 m are dominated by granite densities and a natural gamma radiation that is fairly high, possibly indicating an occurrence of fine-grained granite. Section c. 130–190 m is dominated by high density rocks (diorite to gabbro composition) and low, moderate and high radiation levels. From 190 m down to c. 500 depth there is a dominance of silicate densities indicating a mineral composition corresponding to granodiorite to tonalite rocks with radiation levels of ca 20 µR/h to 30 µR/h. Below 500 m depth there is a dominance of rocks of indicated granite composition with some occurrence of sections of fairly high densities and various gamma radiation levels.

The fracture estimation indicates increased fracturing along a long section starting at c. 400 m depth and ending at c. 565 m depth (Figure 5-23). High fracture frequency is also indicated between 620 m and 675 m depth. Rock alteration is mainly indicated at 445–480 m depth.

6 Discussion and conclusions

A summation of some of the petrophysical parameters gained from KSH02 and KAV01 is presented in Table 6-1. The average values of the petrophysical parameters of the Ävrö granite and the primary fine-grained dioritoid conforms very well to data from previous investigations of these rocks /6, 7/.

It must be noted that the average electric resistivity values presented in Table 6-1 are derived from measurements in normal tap water. For a comparison between sample resistivity data and the resistivity logging of KSH02 we refer to the sample measurements performed in saline water, since the borehole fluid resistivity of KSH02 is very low.

Table 6-1. Average values of some petrophysical parameters from rock samples in KSH02 and KAV01.

Rock type Borehole Comment	Number of samples	Wet density (kg/m3)	Magnetic susceptibility (Logarithm 10^{-5} SI)	Q-value (unit less)	Electric resistivity, fresh water 0.1 Hz (Logarithm Ωm)	Induced polarization, fresh water 0.1 Hz (mrad)	Porosity (%)
Fine-grained dioritoid KSH02 Primary	9	2780±17	3.24±0.53	0.25±0.11	4.42±0.37	8.9±3.3	0.41±0.22
Fine-grained dioritoid KSH02 Plastic deformation	3	2793±3	2.32±1.06	0.34±0.21	4.51±0.37	9.3±2.2	0.32±0.14
Fine-grained dioritoid KSH02 Strong alteration 5 samples for IP and resistivity	6	2717±29	2.22±0.38	0.29±0.11	3.56±0.42	10.1±3.1	2.00±0.85
Fine-grained diorite to gabbro KSH02	3	2851±10	3.84±0.07	0.29±0.16	4.15±0.20	13.4±0.8	0.46±0.11
Ävrö granite KAV01 Primary 9 samples for the average density	7	2686±32	3.29±0.09	0.28±0.21	4.05±0.12	9.8±5.0	0.44±0.05
Fine-grained dioritoid KAV01	2	2830±26	3.47±0.31	0.24±0.04	4.35±0.60	11.2±7.7	0.26±0.21
Fine-grained diorite to gabbro? KAV01 Altered?	3	2863±80	2.49±0.94	0.13±0.06	4.66±0.36	8.7±2.0	0.14±0.06
Granite? Fine- to medium-grained Altered?	1	2701	3.57	0.09	4.60	11.0	0.16

On basis of the results from the petrophysical measurements of KSH02 we conclude that strong alteration clearly affects the physical properties of the fine-grained dioritoid rock. The density, the electric resistivity, the magnetic susceptibility and the remanent magnetization intensity are significantly lower for the altered rock samples, whereas the porosity is higher. Q-values and IP-values in fresh water are unchanged. Altered samples shows a residual IP in saline water indicating electronic conduction in minerals. The unchanged Q-values indicate that the alteration has given rise to a destruction of magnetite but there is no indication of alteration of magnetite to hematite. However, the reddish color of some of the samples and red rims along fractures and possibly the IP in saline water indicates the opposite. Some of the altered samples have fracture fillings of chlorite or epidote, which most likely contributes to the low electric resistivity through surface conductivity. Plastic deformation appears to destroy magnetite, but does not seem to affect the density, the porosity or the electrical properties of the fine-grained dioritoid rock. An analysis of the porosity and resistivity data indicates that the altered samples have significantly different pore space geometry than the primary samples.

The Ävrö granite mainly show typical “granite-densities” and have electrical properties that correspond to primary crystalline rocks typical for the Swedish bedrock.

The rock in the vicinity of KSH02 seems to be dominated by a rock type with a mineral composition that corresponds to tonalite or diorite rocks. The geophysical logging data indicate frequent occurrence of fine-grained granite along the section 500–720 m. Along this section there are indications of increased fracturing. A possible deformation zone is also indicated at c. 280–300 m depth of KSH02. A prominent anomaly in the vertical temperature gradient data at 855 m depth might indicate the occurrence of a water bearing fracture.

The geophysical logging data of KAV01 indicate increased fracturing along large parts of the section at 400–565 m depth. This indication is also supported by the vertical temperature gradient data. The rock in the vicinity of KAV01 is dominated by silicate densities ranging from indicated granite to tonalite mineral composition. The natural gamma radiation intensity is clearly higher along the uppermost 135 m, and also along the section c. 500–600 m, of the borehole than for the other parts of KAV01. This may reflect lithological variations. The density logging data at c. 44–50 m depth should be disregarded (or taken with great care) because of the suspicion of erroneous data.

References

/1/ **Nielsen U T, Ringgaard J, Horn F, 2003.** Geophysical borehole logging in borehole KSH02 and KLX02. SKB P-03-111, Svensk Kärnbränslehantering AB.

/2/ **Mattsson H, Thunehed H, 2003.** Measurements of petrophysical parameters on rock samples during autumn 2002. SKB P-03-19, Svensk Kärnbränslehantering AB.

/3/ **Sehlstedt S, 1988.** Description of geophysical data on the SKB data base GEOTAB. SKB TR 88-05, Svensk Kärnbränslehantering AB.

/4/ **Henkel H, 1991.** Petrophysical properties (density and magnetization) of rock from the northern part of the Baltic Shield. Tectonophysics 192, 1–19.

/5/ **Puranen, R, 1989.** Susceptibilities, iron and magnetite content of precambrian rocks in Finland. Geological survey of Finland, Report of investigations 90, 45 pp.

/6/ **Mattsson H, Thunehed H, 2004.** Interpretation of geophysical borehole data from KSH01A, KSH01B, KSH02 (0–100 m), HSH01, HSH02 and HSH03, and compilation of petrophysical data from KSH01A and KSH01B, SKB P-04-28, Svensk Kärnbränslehantering AB.

/7/ **Mattsson H, Thunehed H, Triumf C A, 2003.** Compilation of petrophysical parameters from rock samples and in situ gamma-ray spectrometry measurements. SKB P-03-97, Svensk Kärnbränslehantering AB.

Appendix 1

Generalized geophysical loggings together with geophysical logging data for the borehole KSH02

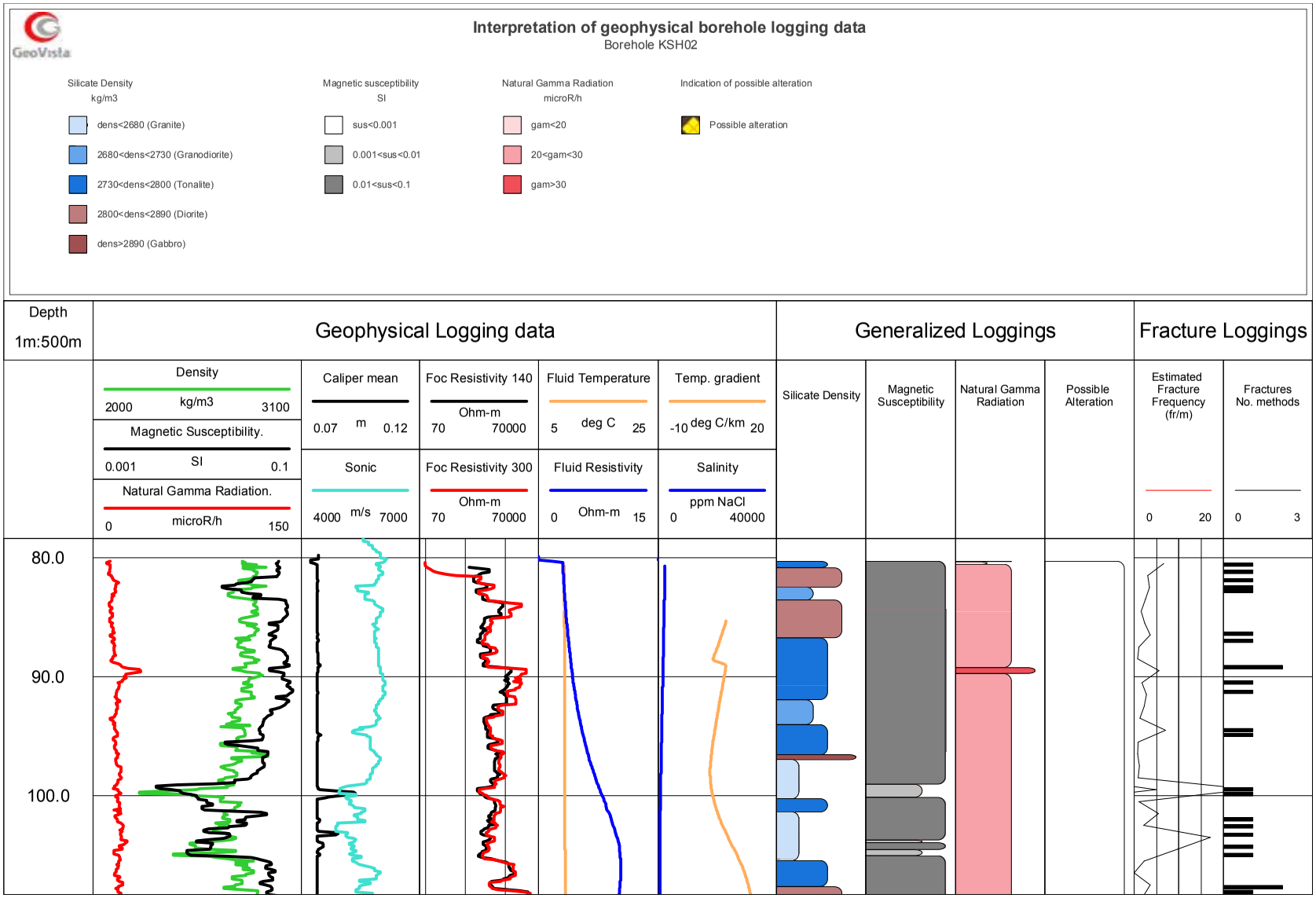
GeoVista
Interpretation of geophysical borehole logging data
Borehole KSH02
Silicate Density
kg/m3
dens<2680 (Granite)
2680<dens<2730 (Granodiorite)
2730<dens<2800 (Tonalite)
2800<dens<2890 (Diorite)
dens>2890 (Gabbro)
Magnetic susceptibility
SI
sus<0.001
0.001<sus<0.01
0.01<sus<0.1
Natural Gamma Radiation
microR/h
gam<20
20<gam<30
gam>30
Indication of possible alteration
Possible alteration
Depth
1m:500m
Geophysical Logging data
Generalized Loggings
Fracture Loggings
Density
2000 kg/m3 3100
Magnetic Susceptibility.
0.001 SI 0.1
Natural Gamma Radiation.
0 microR/h 150
Caliper mean
0.07 m 0.12
Sonic
4000 m/s 7000
Foc Resistivity 140
70 Ohm-m 70000
Foc Resistivity 300
70 Ohm-m 70000
Fluid Temperature
5 deg C 25
Fluid Resistivity
0 Ohm-m 15
Temp. gradient
-10 deg C/km 20
Salinity
0 ppm NaCl 40000
Silicate Density
Magnetic Susceptibility
Natural Gamma Radiation
Possible Alteration
Estimated Fracture Frequency (fr/m)
0 20
Fractures No. methods
0 3
80.0
90.0
100.0

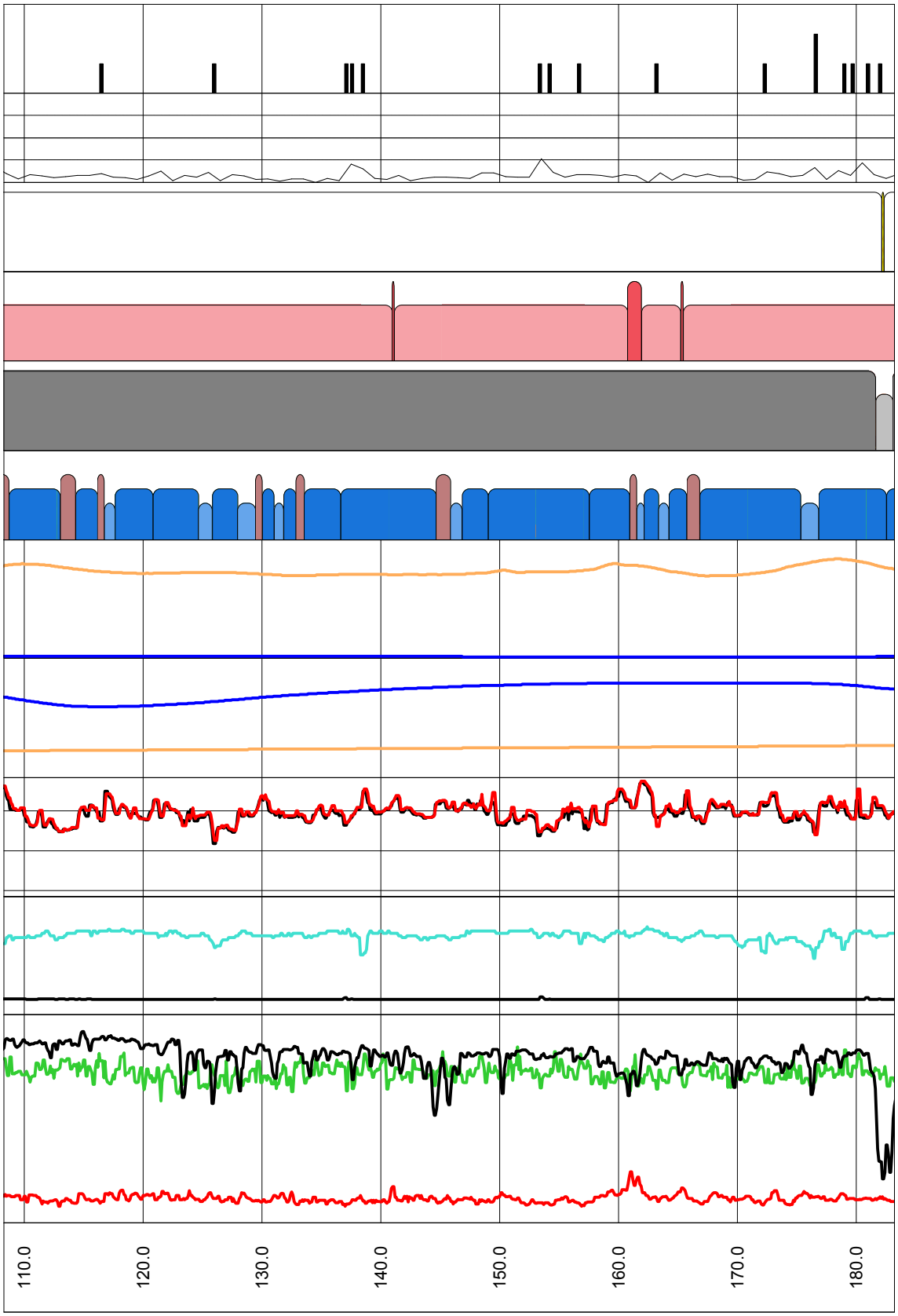
110.0
120.0
130.0
140.0
150.0
160.0
170.0
180.0

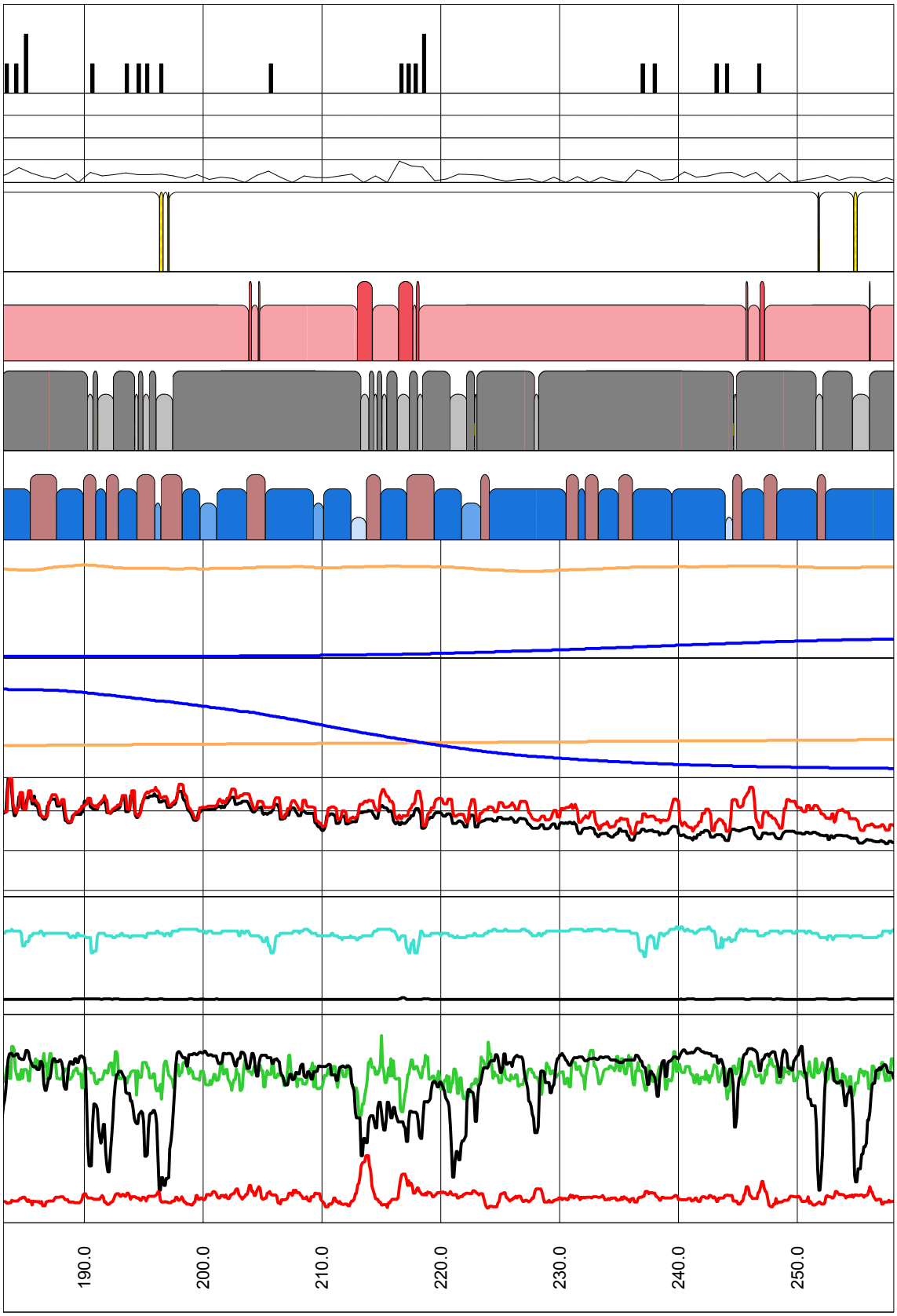
190.0
200.0
210.0
220.0
230.0
240.0
250.0

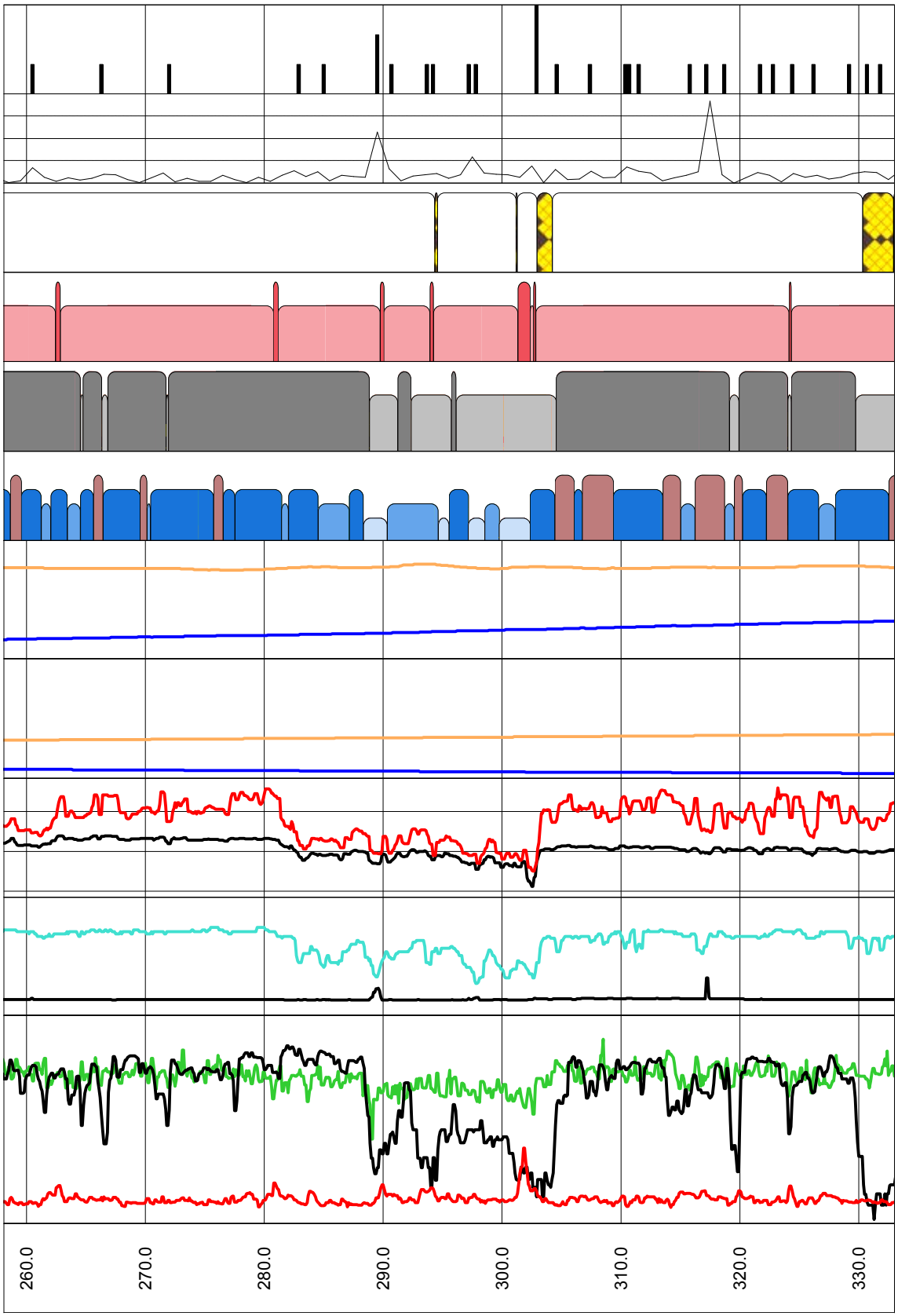
260.0
270.0
280.0
290.0
300.0
310.0
320.0
330.0

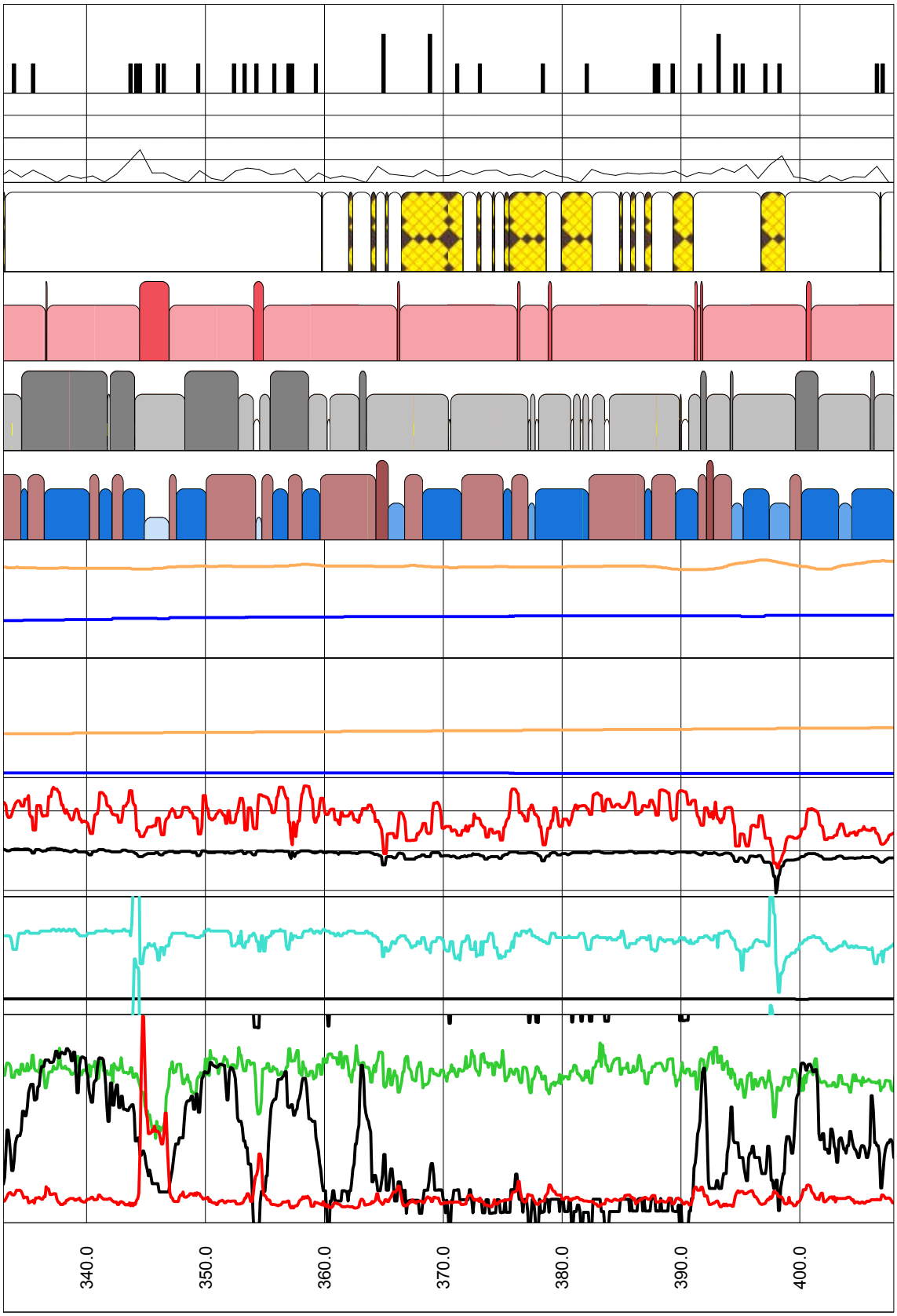
340.0
350.0
360.0
370.0
380.0
390.0
400.0

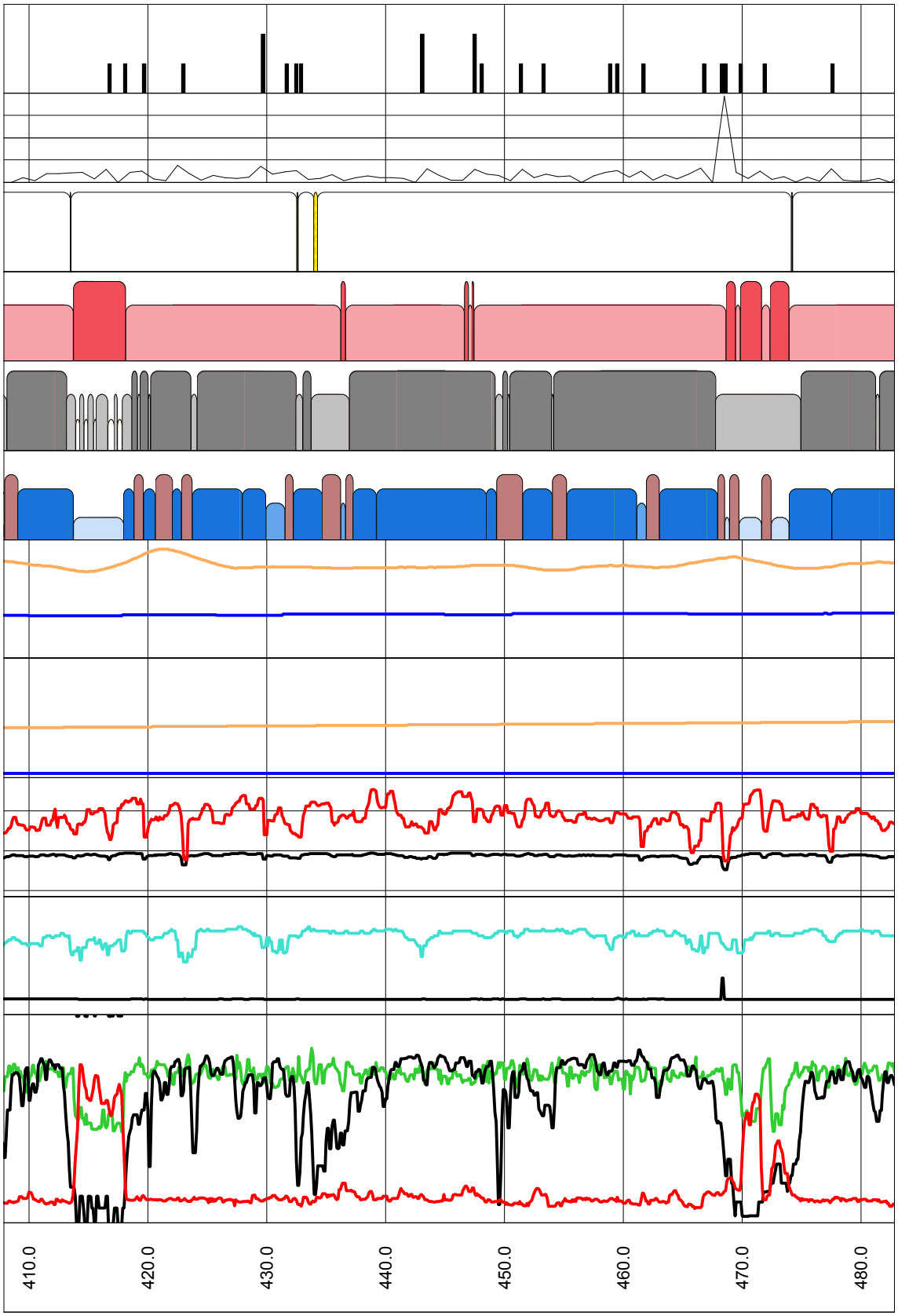
410.0
420.0
430.0
440.0
450.0
460.0
470.0
480.0

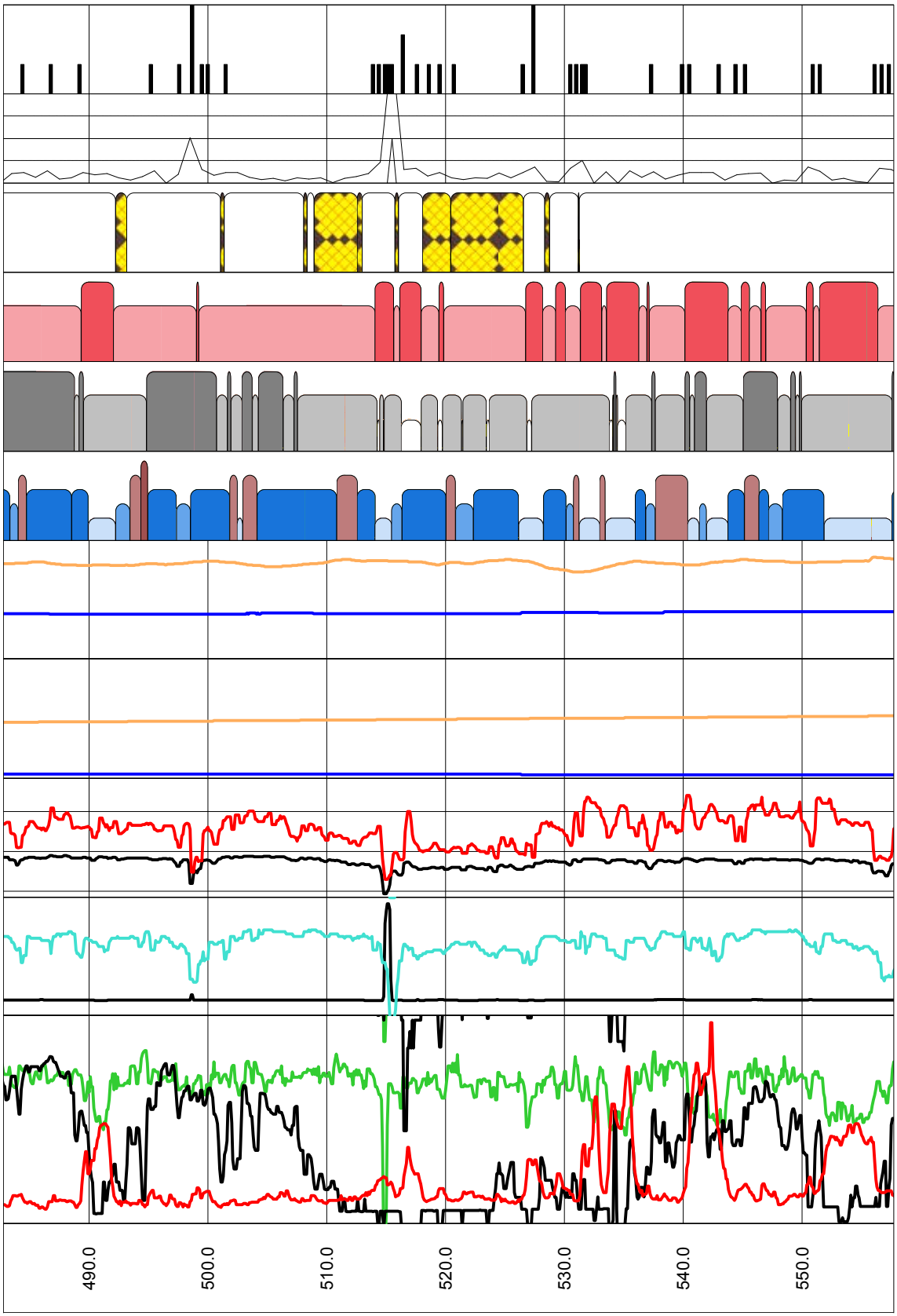
490.0
500.0
510.0
520.0
530.0
540.0
550.0

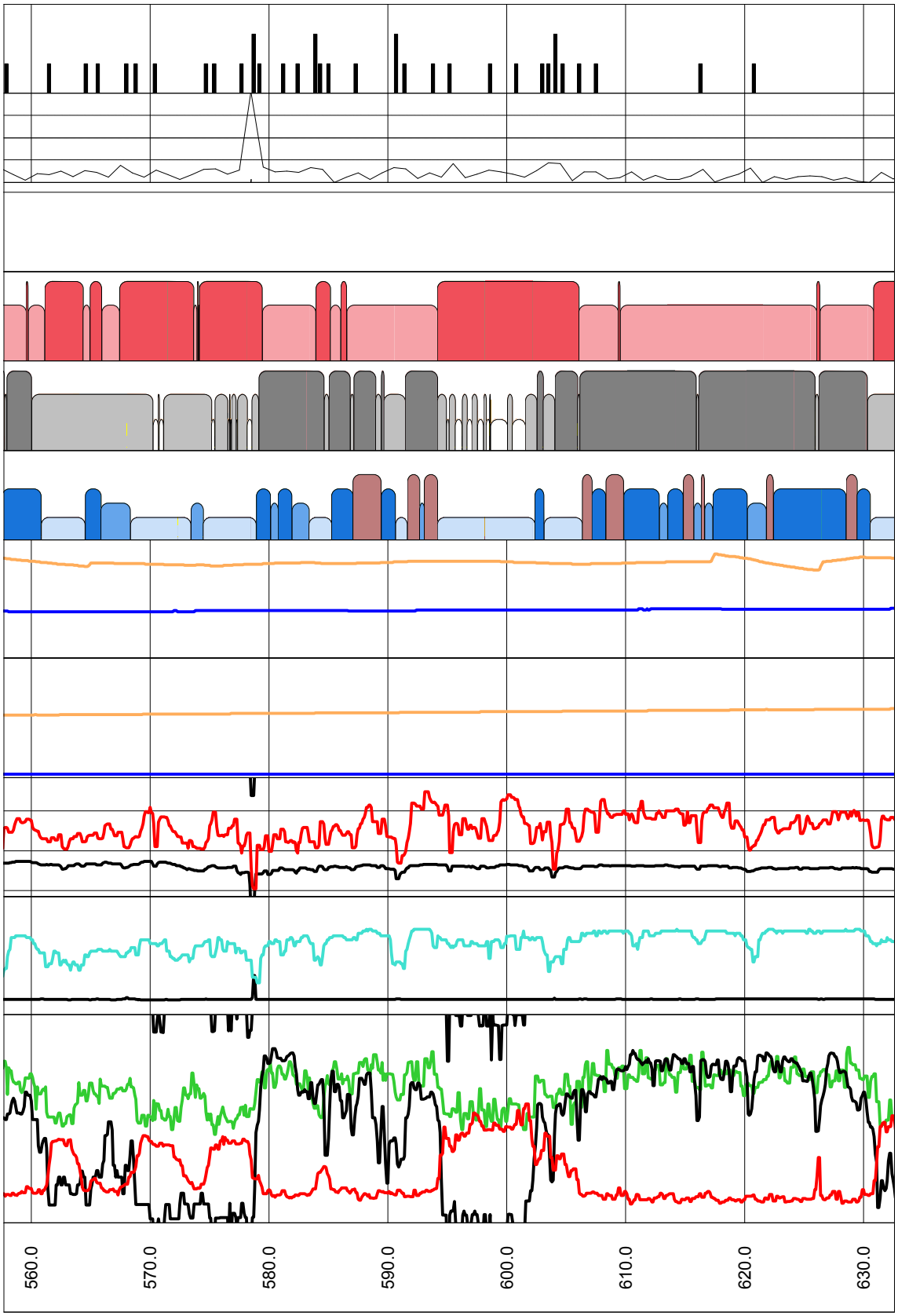
560.0
570.0
580.0
590.0
600.0
610.0
620.0
630.0

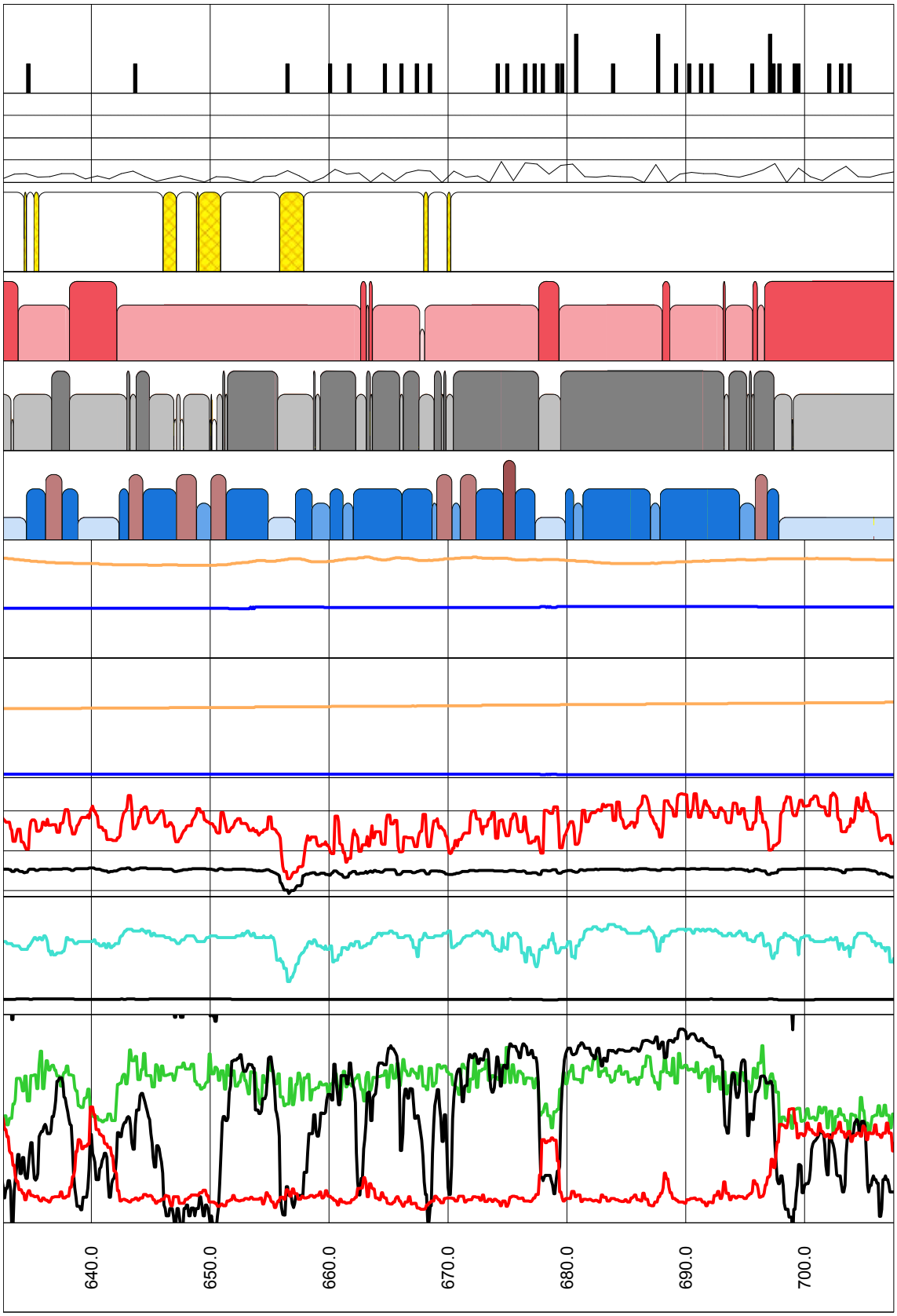
640.0
650.0
660.0
670.0
680.0
690.0
700.0

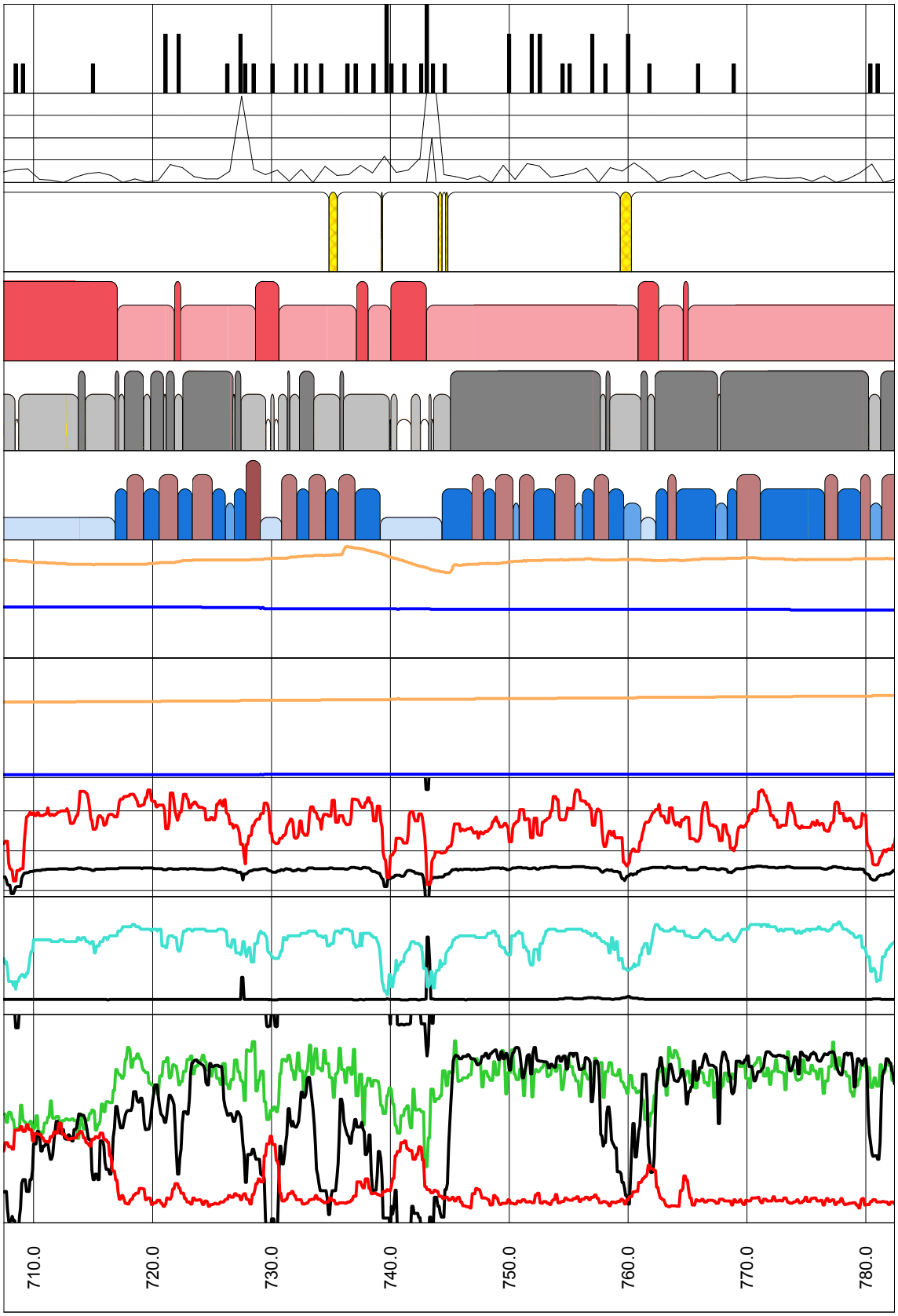
710.0
720.0
730.0
740.0
750.0
760.0
770.0
780.0

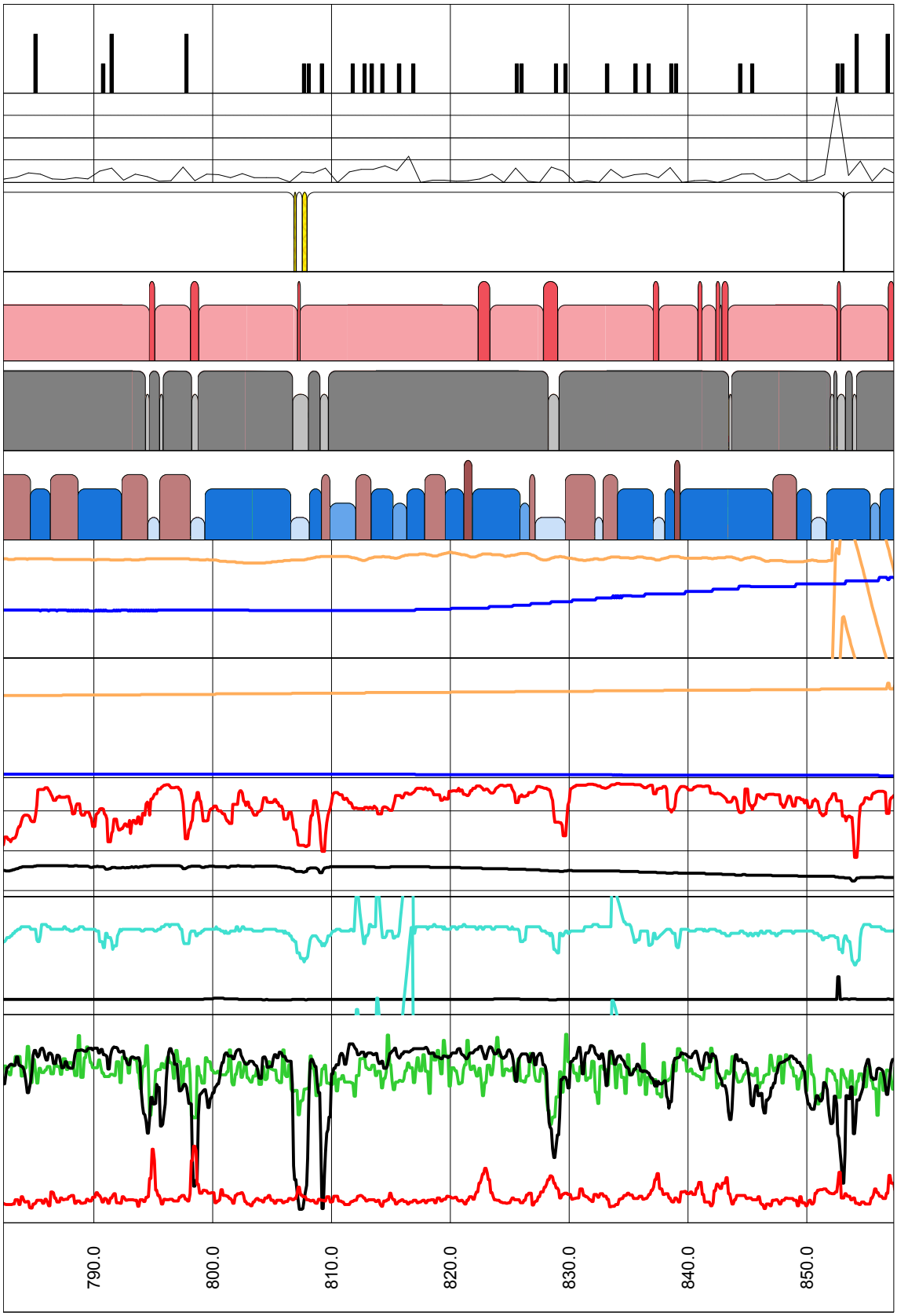
790.0
800.0
810.0
820.0
830.0
840.0
850.0

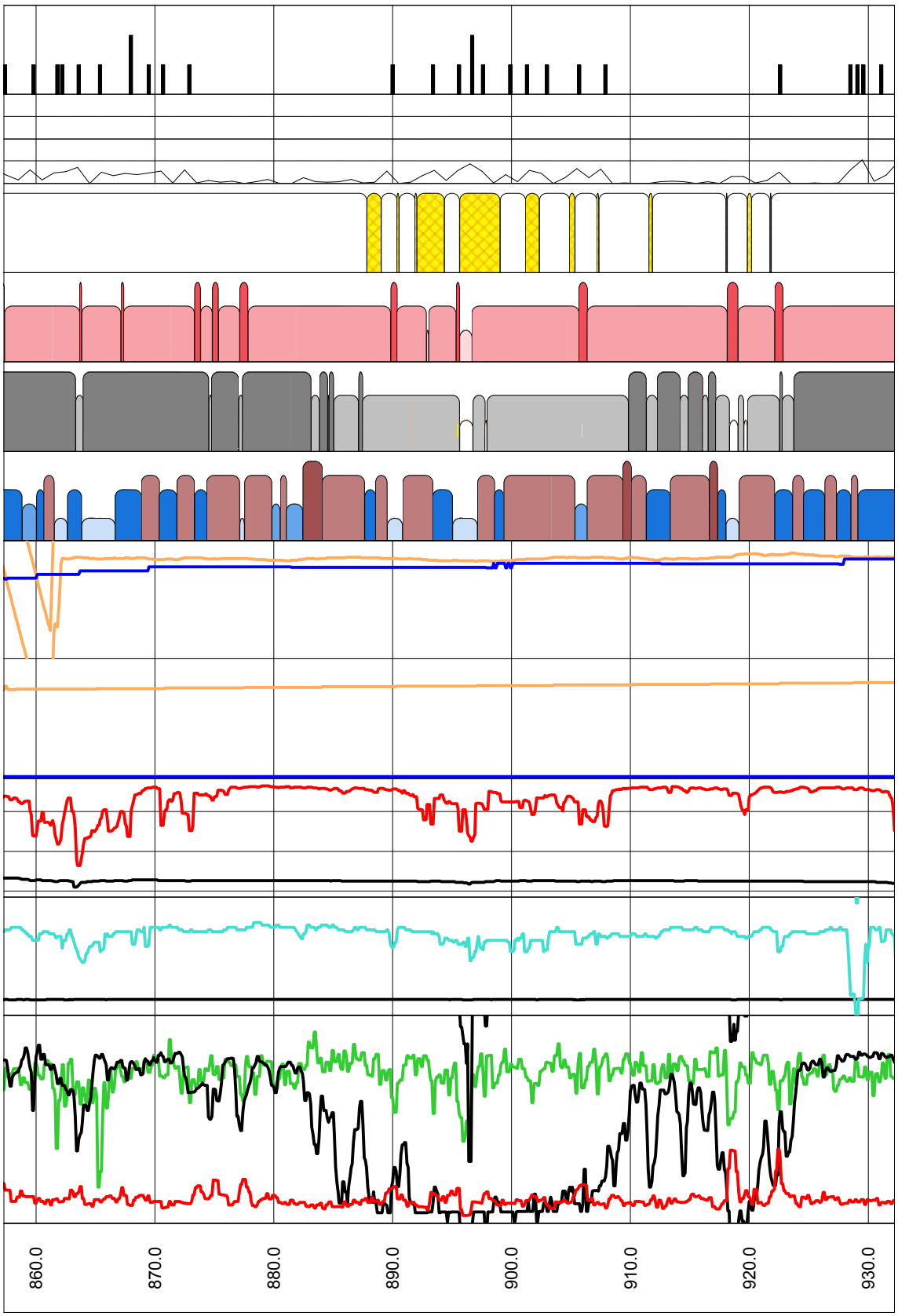
860.0
870.0
880.0
890.0
900.0
910.0
920.0
930.0

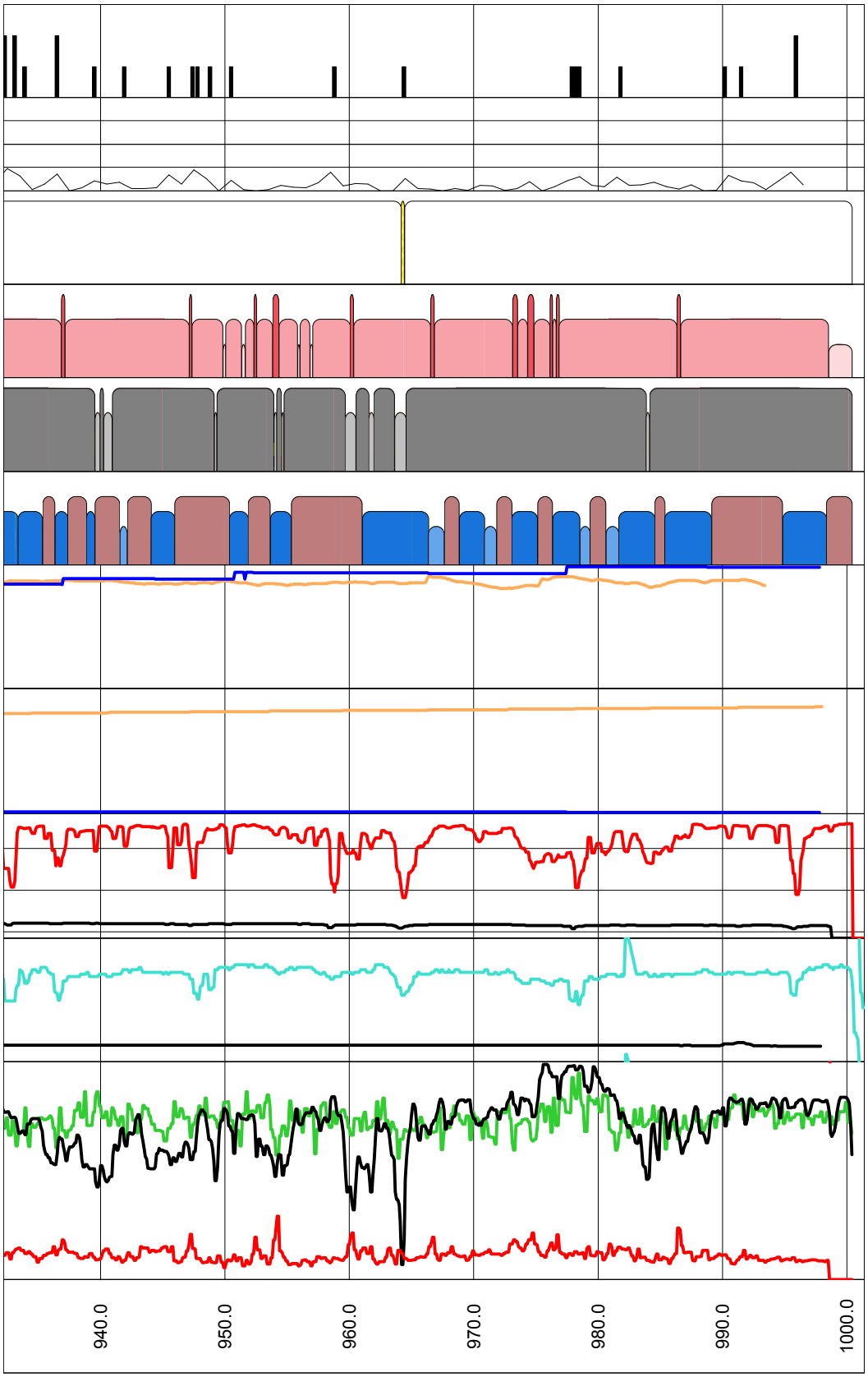
940.0
950.0
960.0
970.0
980.0
990.0
1000.0

Appendix 2

Generalized geophysical loggings together with geophysical logging data for the borehole KAV01

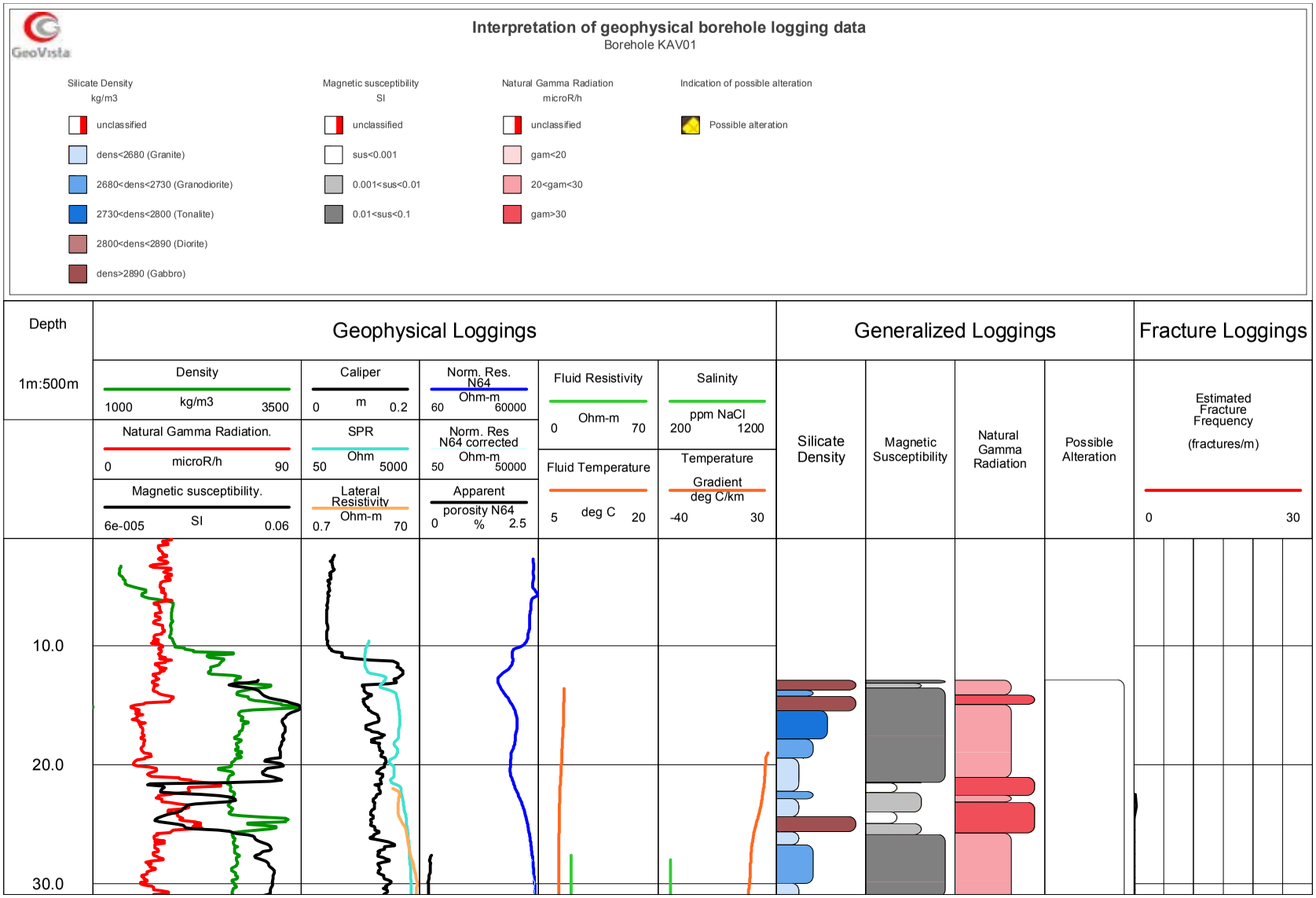
GeoVista
Interpretation of geophysical borehole logging data
Borehole KAV01
Silicate Density
kg/m3
unclassified
dens<2680 (Granite)
2680<dens<2730 (Granodiorite)
2730<dens<2800 (Tonalite)
2800<dens<2890 (Diorite)
dens>2890 (Gabbro)
Magnetic susceptibility
SI
unclassified
sus<0.001
0.001<sus<0.01
0.01<sus<0.1
Natural Gamma Radiation
microR/h
unclassified
gam<20
20<gam<30
gam>30
Indication of possible alteration
Possible alteration
Depth
1m:500m
Geophysical Loggings
Generalized Loggings
Fracture Loggings
Density
1000 kg/m3 3500
Caliper
0 m 0.2
Norm. Res. N64
60 Ohm-m 60000
Fluid Resistivity
0 Ohm-m 70
Salinity
200 ppm NaCl 1200
Natural Gamma Radiation.
0 microR/h 90
SPR
50 Ohm 5000
Norm. Res N64 corrected
50 Ohm-m 50000
Fluid Temperature
5 deg C 20
Temperature Gradient
-40 deg C/km 30
Magnetic susceptibility.
6e-005 SI 0.06
Lateral Resistivity
0.7 Ohm-m 70
Apparent porosity N64
0 % 2.5
Silicate Density
Magnetic Susceptibility
Natural Gamma Radiation
Possible Alteration
Estimated Fracture Frequency
(fractures/m)
0 30
10.0
20.0
30.0

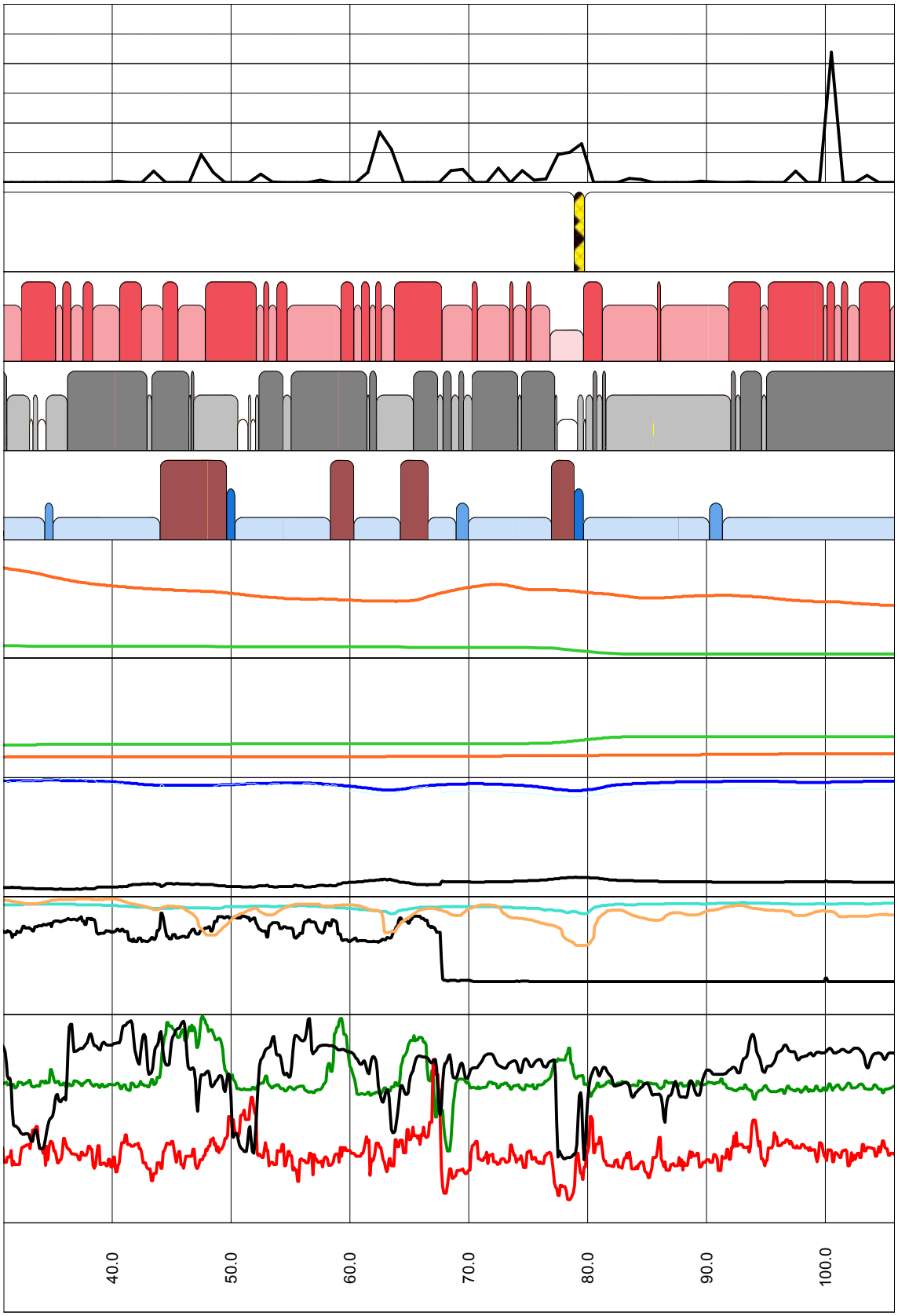
40.0
50.0
60.0
70.0
80.0
90.0
100.0

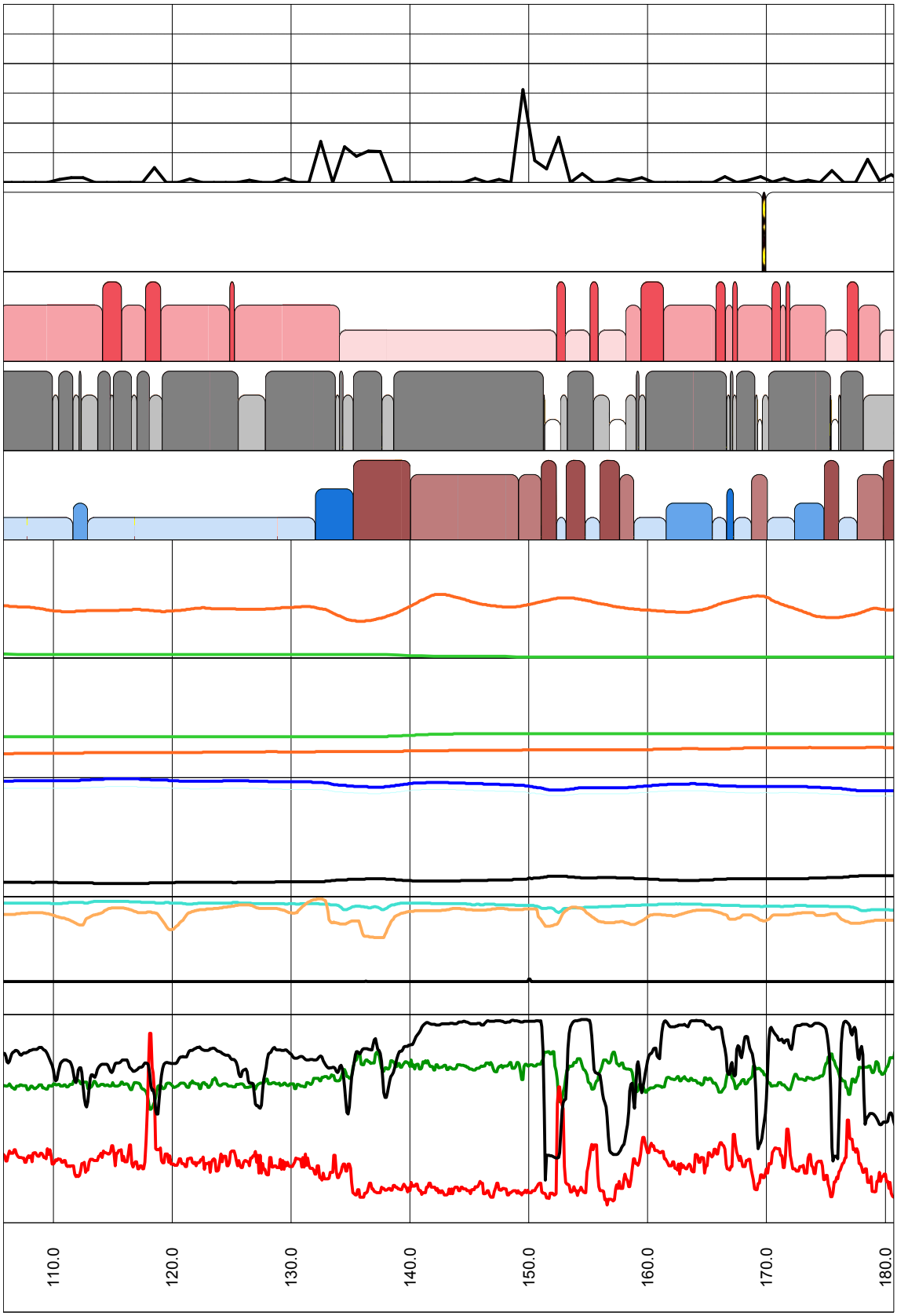
110.0
120.0
130.0
140.0
150.0
160.0
170.0
180.0

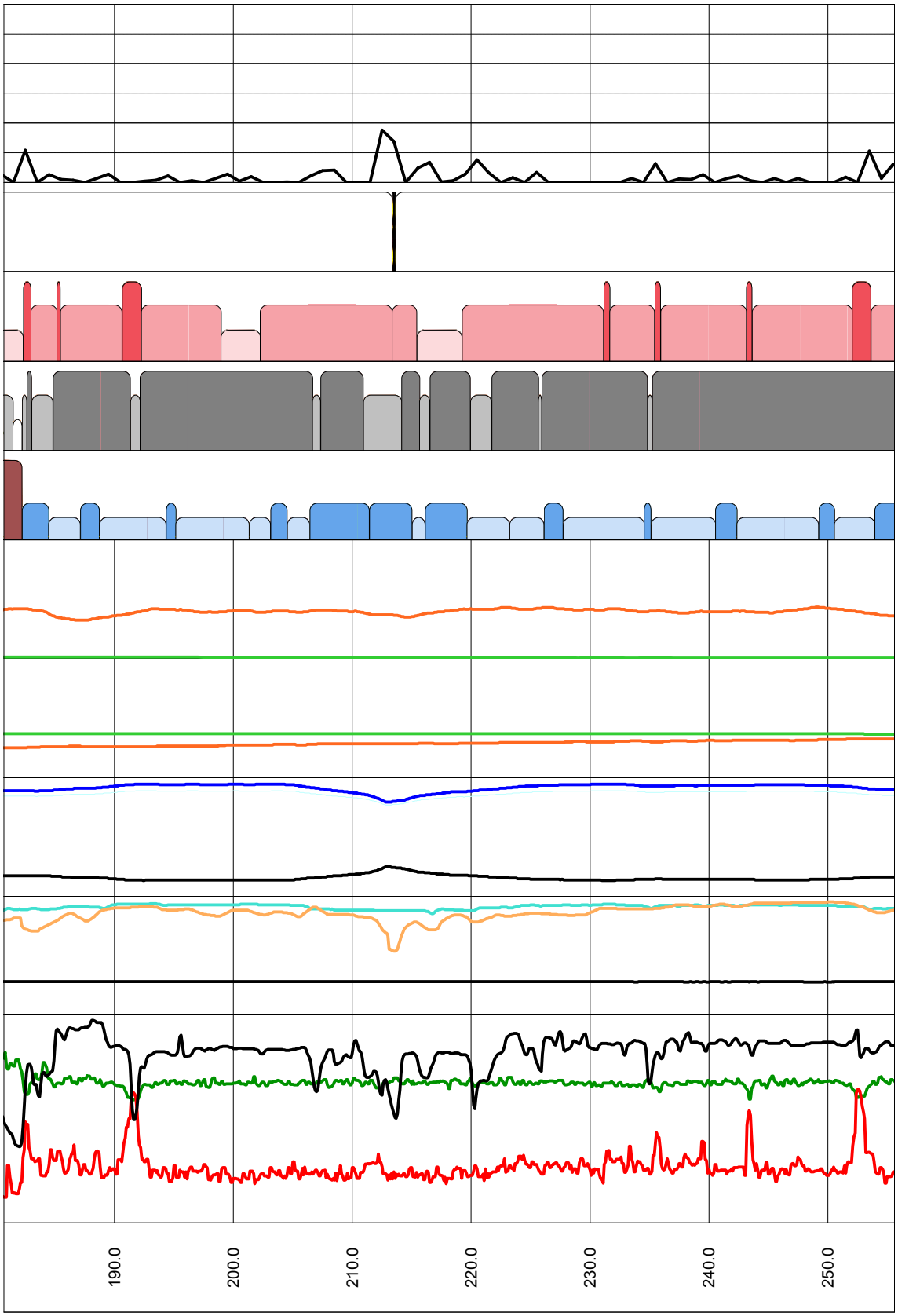
190.0
200.0
210.0
220.0
230.0
240.0
250.0

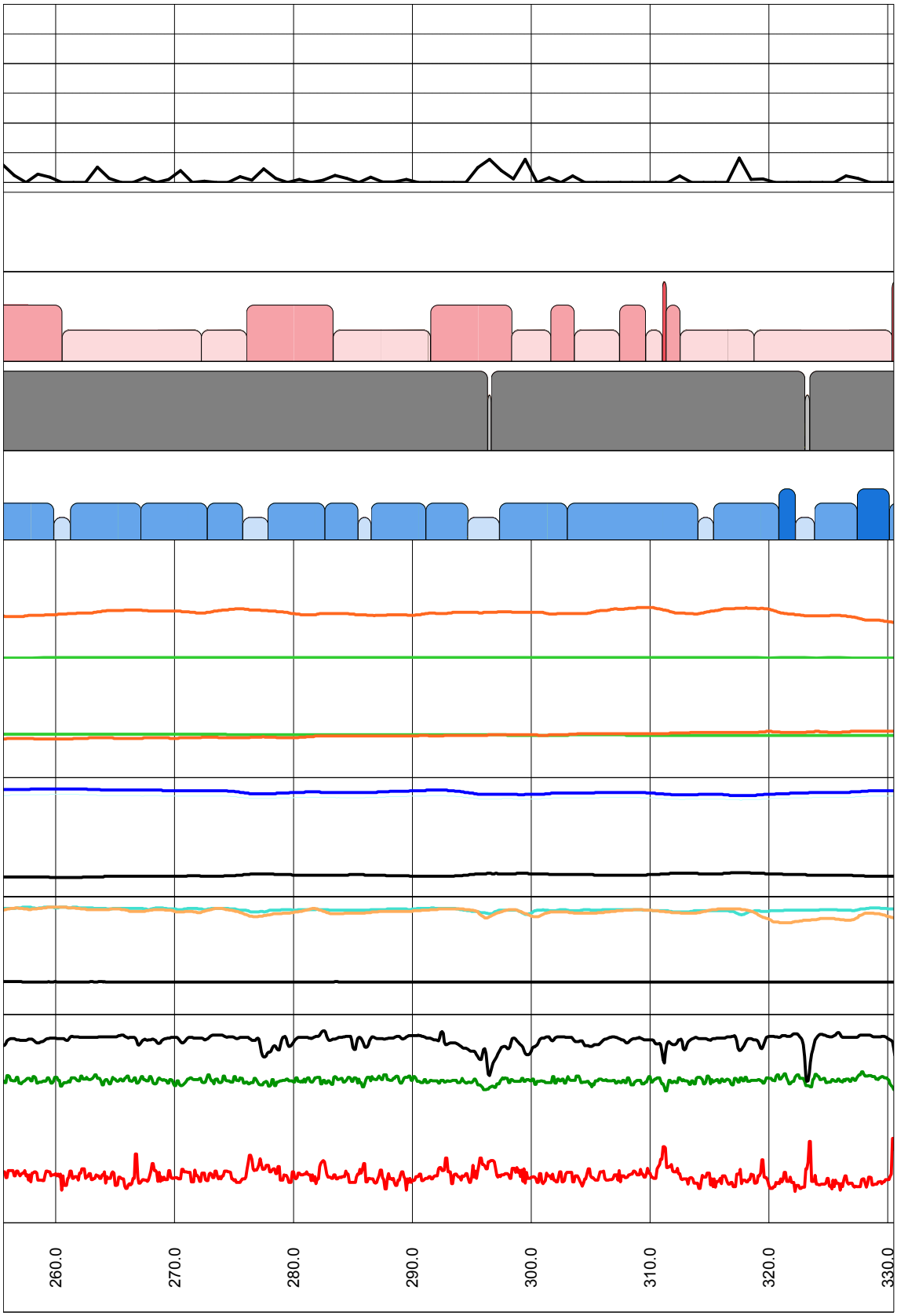
260.0
270.0
280.0
290.0
300.0
310.0
320.0
330.0

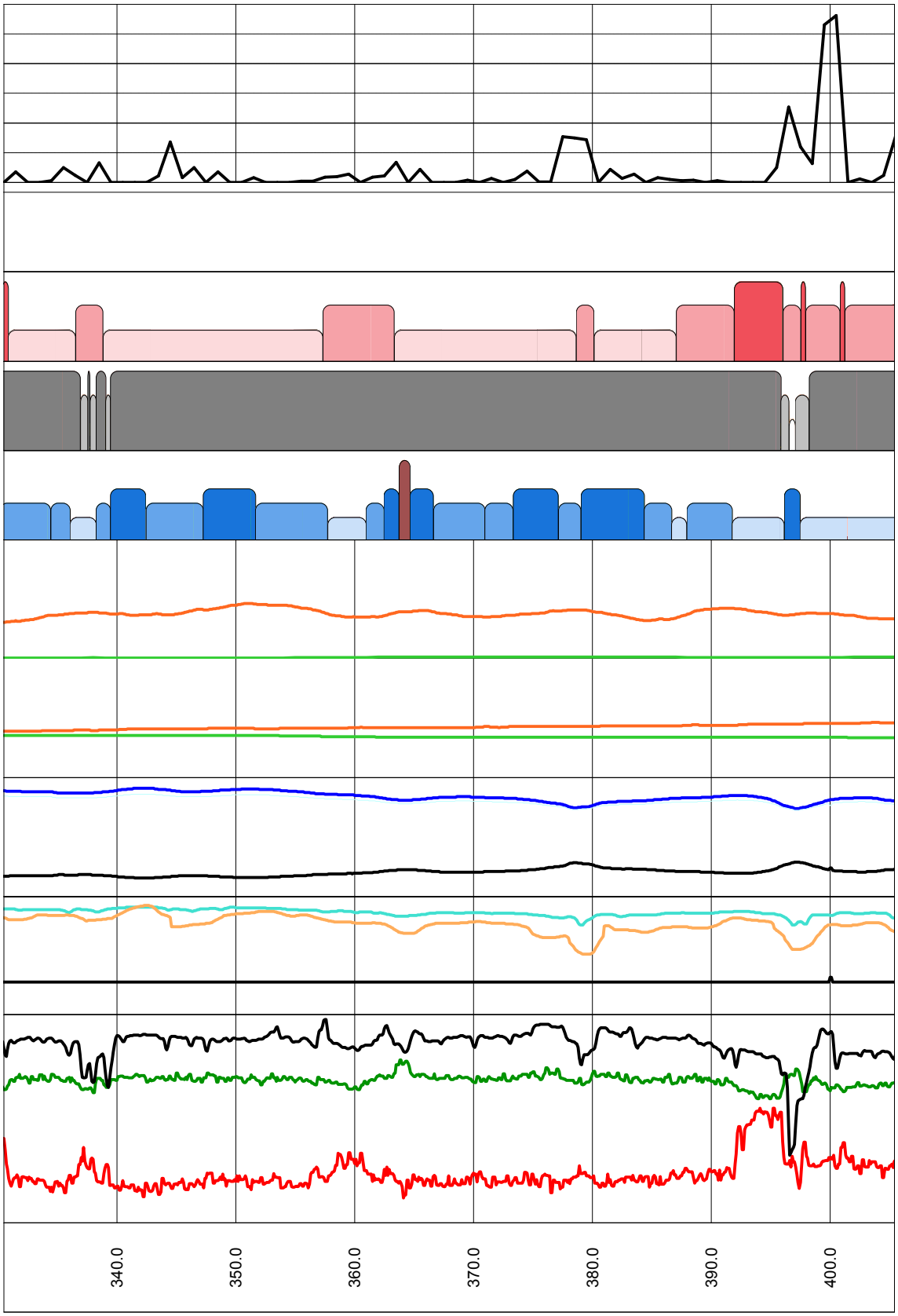
340.0
350.0
360.0
370.0
380.0
390.0
400.0

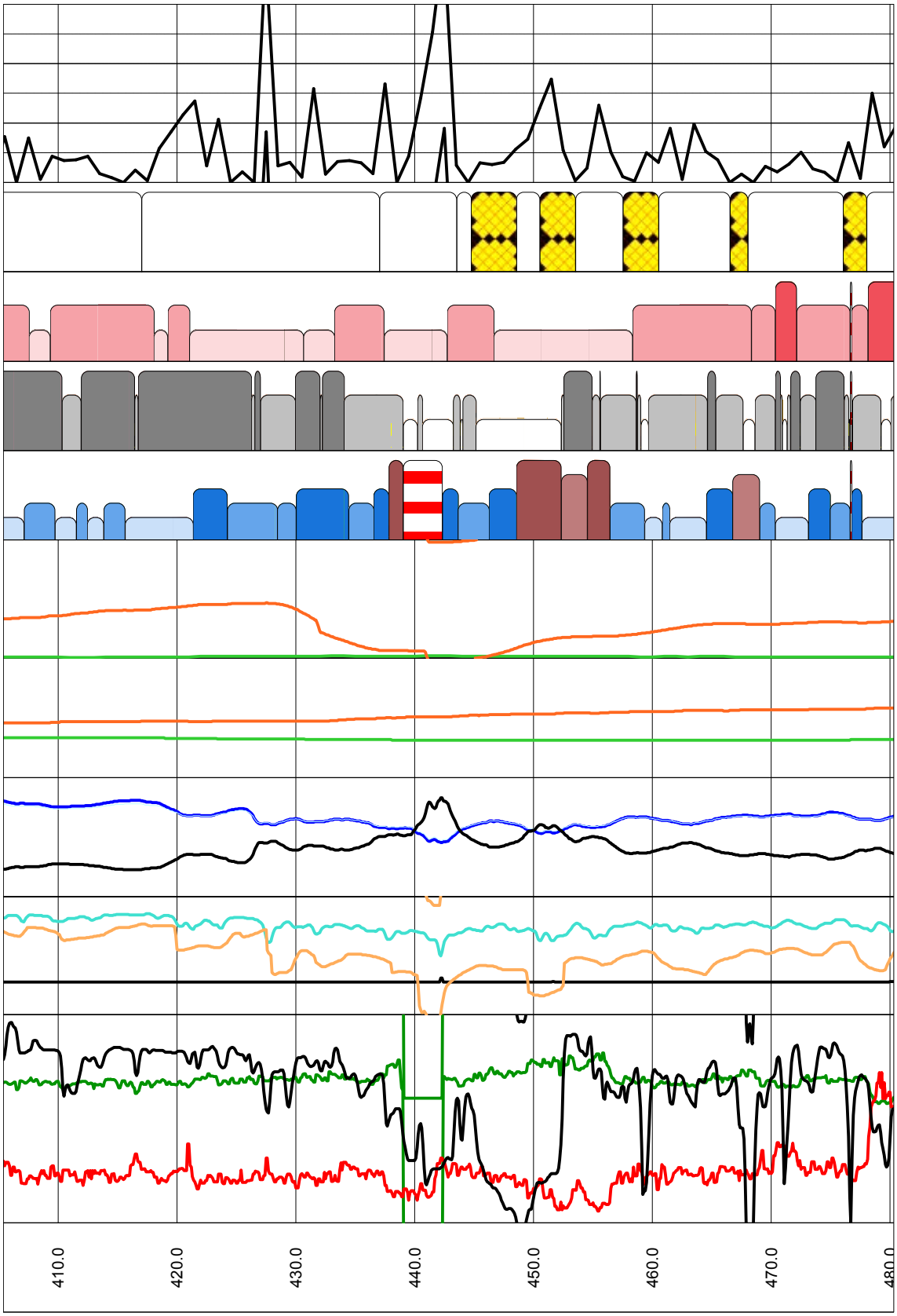
410.0
420.0
430.0
440.0
450.0
460.0
470.0
480.0

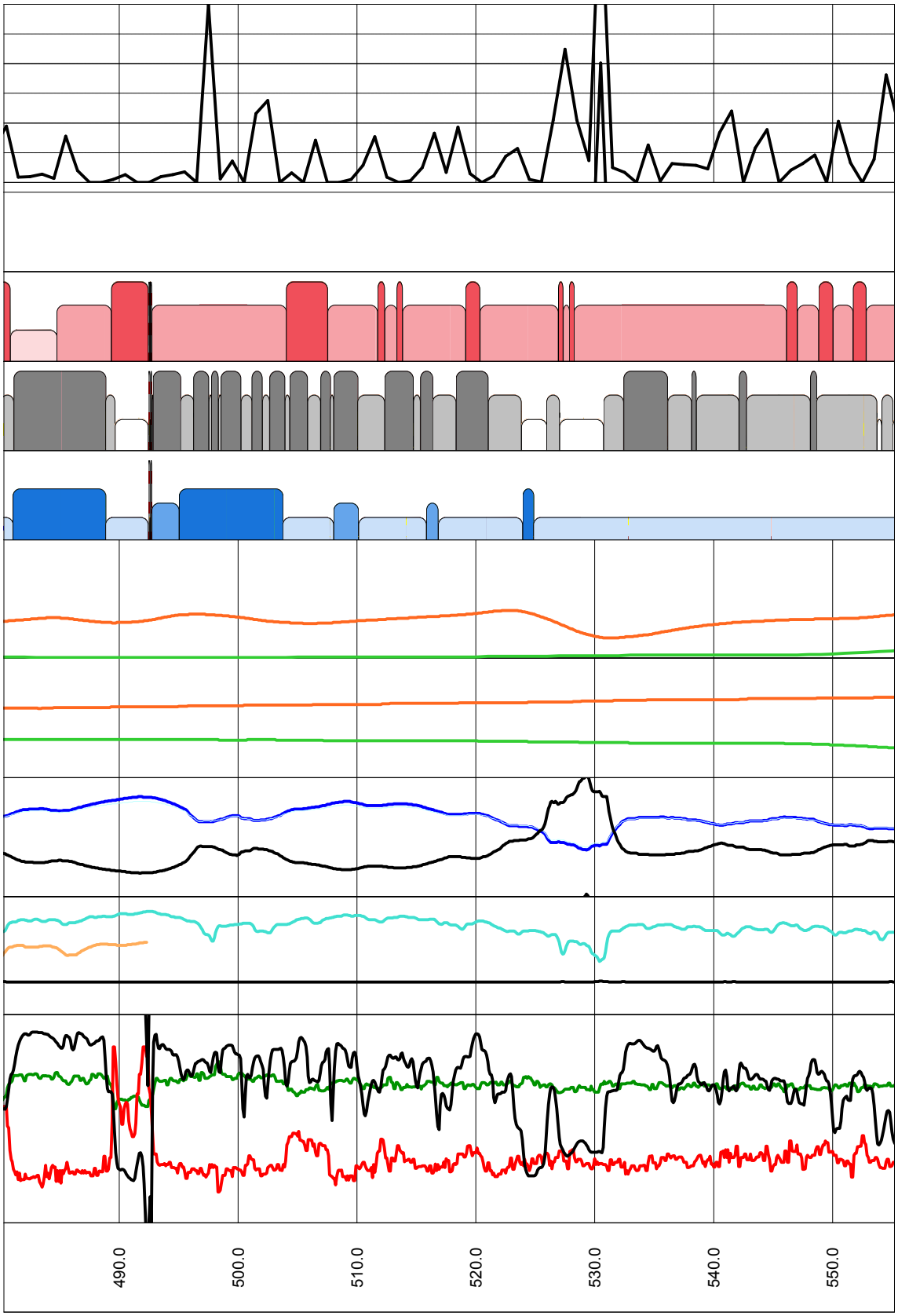
490.0
500.0
510.0
520.0
530.0
540.0
550.0

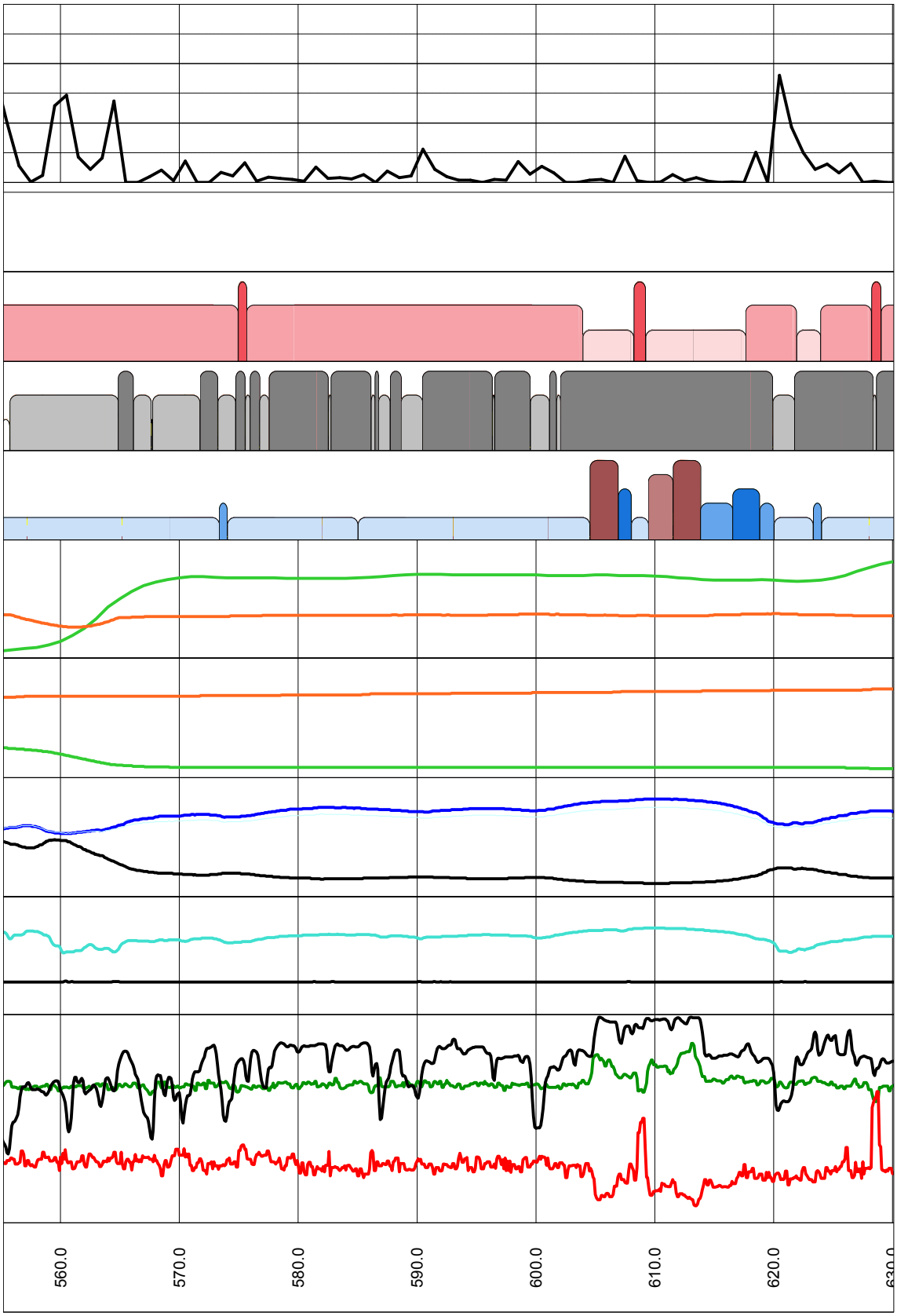
560.0
570.0
580.0
590.0
600.0
610.0
620.0

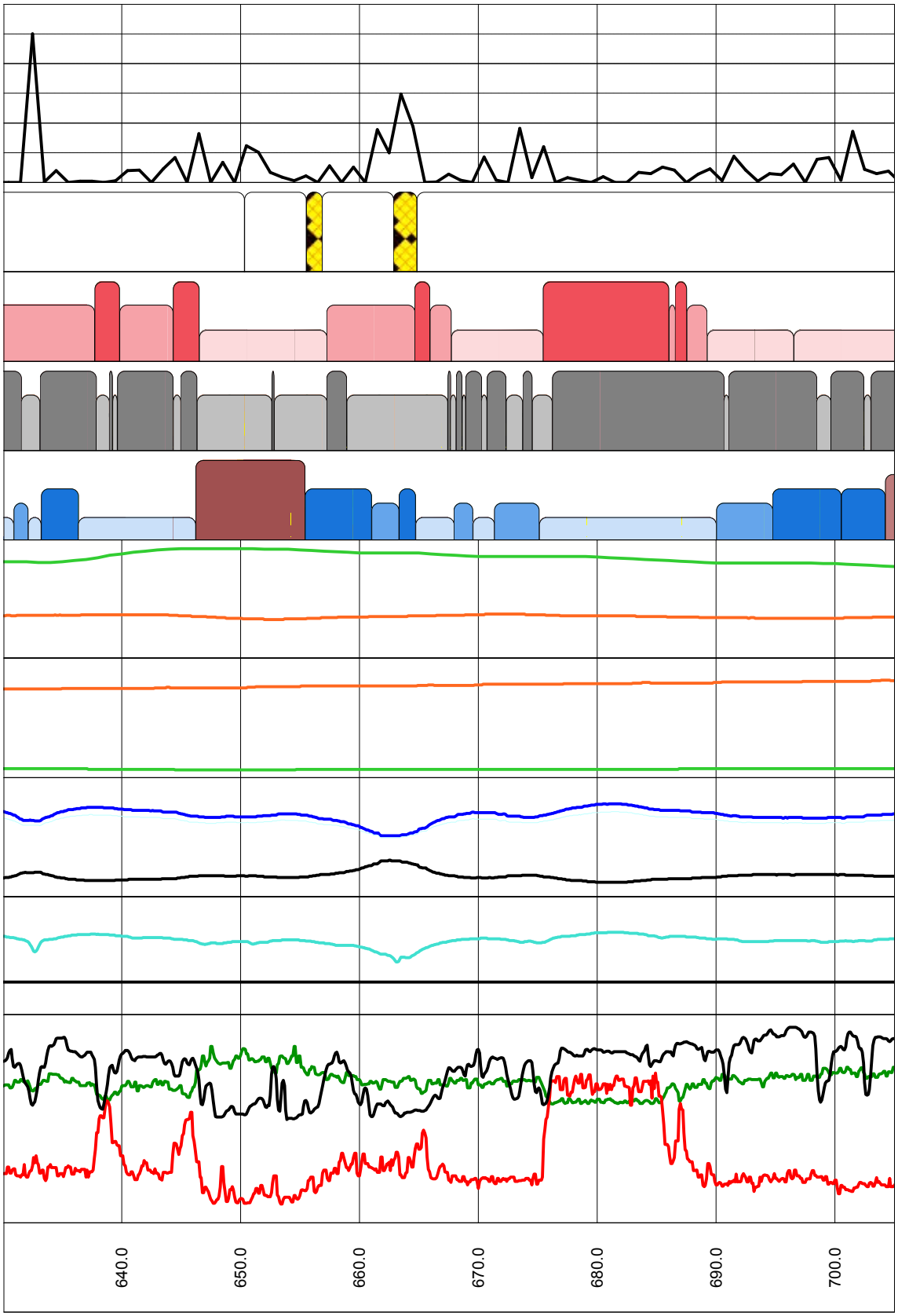
640.0
650.0
660.0
670.0
680.0
690.0
700.0

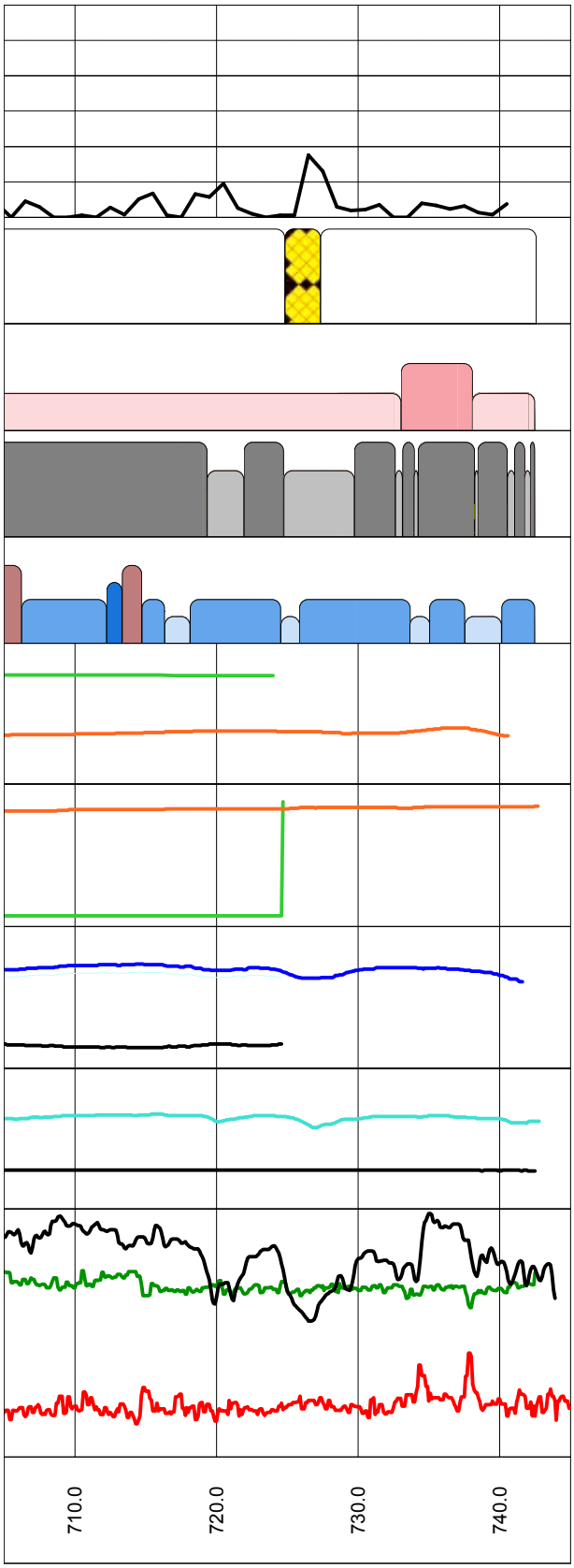
710.0
720.0
730.0
740.0